Reactive and Functional Polymers 217 (2025) 106492

Contents lists available at ScienceDirect

Reactive and Functional Polymers

journal homepage: www.elsevier.com/locate/react

Reaction routes with glycidyl methacrylate for the incorporation of oleic acid in amphiphilic block copolymers

Catarina P. Gomes [a], Mário Rui P.F.N. Costa [b], Rolando C.S. Dias [a,*]

[a] Centro de Investigação de Montanha (CIMO), Instituto Politécnico de Bragança, Campus de Santa, Apolónia, 5300-253 Bragança, Portugal
[b] LSRE, Faculdade de Engenharia da Universidade do Porto, Rua Roberto Frias s/n, 4200-465 Porto, Portugal

ARTICLE INFO

Keywords:
Glycidyl methacrylate
Oleic acid
Amphiphilic block copolymers
Self-assembly
Encapsulation

ABSTRACT

This research focused on assessing different reaction routes for synthesizing amphiphilic block copolymers, with the hydrophobic part built using glycidyl methacrylate and oleic acid and the hydrophilic segment made from 2-(dimethylamino)ethyl methacrylate. The main objectives of this study were to identify reaction routes leading to low-impact branching and/or crosslinking mechanisms involving epoxides and oleic acid, and to synthesize p(GMA-OA)-*b*-p(DMAEMA) copolymers in a simple and scalable manner. Block copolymer synthesis was considered using both ATRP and RAFT polymerization.

The reaction route involving the synthesis of methacrylated oleic acid proved problematic, whereas higher synthesis efficiency was achieved when the glycidyl methacrylate moieties were modified with oleic acid after polymerization. It was found that working with DMSO solvent and a stoichiometric excess of oleic acid was particularly important for reducing branching/crosslinking. FTIR and GPC analyses were used to assess the progress of the chemical composition and molecular architecture of the intermediate homo- and *co*-polymers, and to demonstrate the successful production of the intended p(GMA-OA)-*b*-p(DMAEMA) materials.

The synthesized block copolymers were used for encapsulating and delivering oleanolic acid considering solid polymer dispersions and aqueous particle dispersions. SEM and TEM analysis demonstrate the ability of the p(GMA-OA)-*b*-p(DMAEMA) copolymers to self-assemble in an aqueous environment and well-defined spherical aggregates were observed, for example with size up to 100 nm in size with an external shell around 5–8 nm thick. A high loading capacity for oleanolic acid was measured, with a range of up to 0.17 mg/mL in aqueous particle dispersions. The dynamics of oleanolic acid release was measured under different conditions, including changes in solvent composition, pH and temperature. The results demonstrate sustained release of the encapsulated oleanolic acid and transitions induced by pH/temperature changes.

1. Introduction

The presence of both vinyl and epoxy reactive groups makes the glycidyl methacrylate (GMA) monomer a versatile starting chemical for synthesizing other tailored monomers, or for producing GMA-based polymers that can be further functionalized through post-polymerization modification [1]. Nowadays, this reactive chemical system has gained significant importance in the production of epoxy-functional methacrylic resins for use as coatings and adhesives, due to the potential incorporation of vegetable oil macromonomers and/or fatty acids (FA) into the final products [2–7]. Indeed, the demand for the reducing or replacing of petroleum-derived raw materials in these industries lead to solutions considering for instance the creation of methacrylated derivatives of fatty acids through the catalytic addition of the epoxy group of GMA to the carboxylic acid group of the FA (epoxy ring opening reaction). This approach was used to synthesize vinyl monomers incorporating oleic acid (OA), lauric acid, myristic acid, stearic acid and others [2–7]. These monomers were then polymerized through free radical mechanisms to generate different products with a range of applications [8–11]. The epoxy ring-opening mechanism involving the moieties of poly(glycidyl methacrylate)-based polymers with multiple functional groups, such as amine, thiol, azide and carboxylic acid groups, as well as hydrolysis reactions, has also been considered in post-polymerization modification approaches for synthesizing a variety of customized functional polymers [1,12]. The development of chromatographic stationary phases is an important

* Corresponding author.
E-mail address: rdias@ipb.pt (R.C.S. Dias).

https://doi.org/10.1016/j.reactfunctpolym.2025.106492
Received 17 August 2025; Received in revised form 19 September 2025; Accepted 22 September 2025
Available online 23 September 2025

application field for GMA-based polymers of this sort. Chemical modification of the epoxy groups enables amino, hydroxyl or thiol groups, among others, to be introduced into polymer particles, providing the selectivity and stability required for the analytical separation of many different compounds [13–16].

Interestingly, the widespread adoption of reversible-deactivation radical polymerizations techniques (RDRP) such as atom transfer radical polymerization (ATRP) and reversible addition–fragmentation chain transfer (RAFT) polymerization has resulted in the creation of GMA-based block copolymers and analogues with other functional groups for use in encapsulation, drug delivery, surface modification and other areas of materials science [17,18]. In this context, well-defined amphiphilic poly(glycidyl methacrylate)-*b*-poly(poly(ethylene glycol) methacrylate) diblock copolymers were recently synthesized using a recyclable photoRDRP mechanim [19]. Block copolymers involving GMA are also possible through living ionic polymerization [20], but controlled radical polymerization permits the use of less stringent reaction conditions to produce a variety of tailored molecular architectures.

It is well established that a multitude of competitive mechanisms are possible for the reactions of glycidyl/epoxy groups with alcohols or carboxylic acids, among other reagents [21]. In the context of the reaction between glycidyl metacrylate and fatty acid carboxylic groups, there is the possibility of a secondary reaction involving epoxides with the formed hydroxyl groups. This secondary reaction is more likely to occur as the carboxylic acid groups are depleted [9,21]. Therefore, species with a high number of reactive centers can be formed in processes involving the transformation of epoxy groups, with the aim of functionalizing GMA monomers or post-modifying polymers containing GMA moieties. Consequently, branching and/or crosslinking mechanisms are possible in such synthesis routes leading to the potential formation of an insoluble fraction in the resulting materials [9]. While a moderate level of branching/crosslinking is acceptable for some applications, such as the production of coatings and adhesives, it can have a detrimental effect on the properties of materials used in other fields, such as those involving well-defined block copolymers.

This study focuses on analyzing various reaction pathways involving glycidyl methacrylate, with the aim of incorporating oleic acid into amphiphilic block copolymers. The ultimate objective is to synthesize hybrid synthetic-natural block copolymers comprising a hydrophobic block resulting from the reaction between OA and the epoxy groups of GMA and a hydrophilic poly(2-(dimethylamino)ethyl methacrylate) block that can be stimulated by changes in pH and/or temperature. The synthesis routes that lead to more straightforward and scalable production of p(GMA-OA)-*b*-p(DMAEMA) copolymers are analyzed, as is the use of these materials for encapsulating and delivering hydrophobic molecules. This research also examines reaction routes that lead to a low enough impact of branching and/or crosslinking mechanisms involving epoxides, in order to prevent unwanted effects on the molecular architecture and end-use properties of the desired materials.

Nowadays, the use of many different drug delivery vehicles is being considered for various applications with the aim of enhancing biological activity against numerous diseases [22–27], including utilization in plants [28–31]. The present work uses oleanolic acid, a pentacyclic triterpenoid found in many plants including the olive tree, where it occurs alongside oleic acid, as a model hydrophobic drug to examine the encapsulation and delivery properties of the p(GMA-OA)-*b*-p(DMAEMA) copolymers that have been developed.

2. Materials and methods

2.1. Materials

All chemicals were used as purchased, without further purification. CuBr (97 % purity), 4-(dimethylamino)pyridine (DMAP, purity≥99 %), 2-(dimethylamino)ethyl methacrylate (DMAEMA, 98 % purity), poly (ethylene glycol) methyl ether of MW 2000 (mPEG 2000), (hydroxyethyl)methacrylate (HEMA, 99 % purity), 2-cyano-2-propyl dodecyl trithiocarbonate (CPDT), ethyl 2-bromopropionate (EBrP, 99 % purity), 9-(diethylamino)-5H-benzo[*a*]phenoxazin-5-one (Nile Red), N,N,N′,N″,N″-pentamethyldiethylenetriamine (PMDETA, 99 % purity) and styrene (purity≥99 %) were purchased from Sigma-Aldrich. α-bromoisobutyryl bromide (BIBB, 98 % purity), 2,2′-bipyridine (BPY, 99 % purity), dicyclohexylcarbodiimide (DCC, 99 % purity), 2-methylimidazole (2MI, 99 % purity) were purchased from Thermo Scientific Chemicals. 3.5 k MWCO cellulose dialysis bag was purchased from Thermo Fisher Scientific. Triethylamine (TEA, 99.5 % purity), glycidyl methacrylate (GMA, 97 % purity), oleanolic acid (97 % purity) were purchased from Acros Organics. *N*,*N*-dimethylformamide (DMF), acetic acid (AcOH), methanol (MeOH), ethanol (EtOH), diethyl ether, hexane and tetrahydrofuran (THF) solvents were purchased from Fisher Chemical while, dimethyl sulfoxide (DMSO) was purchased from Fisher BioReagents. Anisole and 2,2′-azobis(2-methylpropionitrile) (AIBN), were purchased from Fluka Analytical, *S*,*S*-dibenzyltrithiocarbonate (DBZT, 97 % purity) was purchased from Strem Chemicals and oleic acid (OA, 99 % purity), was purchased from Alfa Aesar. Unless otherwise mentioned below, all the reactants and solvents were used as received. The water used in the experiments is ultrapure water supplied by the local laboratory (Millipore water, Milli-Q quality).

2.2. Synthesis of methacrylated oleic acid through reaction with glycidyl methacrylate

The synthesis of methacrylated oleic acid (MOA) through reaction with glycidyl methacrylate was performed in accordance with the principles reported in previous related works on this subject [2–11]. As detailed below, the set of reactions performed included changes in temperature (between 45 and 100 °C), composition of the initial mixture (e.g. molar ratio of GMA/OA between 0.5 and 1.1 as presented in Table 1), presence or absence of catalyst and solvent, and reaction time (e.g. between 5 and 72 h). Briefly, the prescribed amounts of OA, GMA, the 2MI catalyst and the solvent were mixed and allowed to react with stirring for the defined time period. FTIR analysis was used to measure the consumption of epoxy groups of GMA for the different products, using the 910 cm^{-1} assignment as a reference.

Table 1
Different working conditions considered for the synthesis of methacrylated oleic acid through reaction with glycidyl methacrylate. The catalyst amount is presented as the mass fraction relative to sum of GMA and OA content while the solvent amount is expressed as the mass ratio considering also the sum of GMA and OA amount as reference.

Run	Molar ratio GMA/OA	Catalyst (%)	Solvent and mass ratio to GMA + OA		T (°C)	Reaction time (h)
1	1.1	–	–	–	100	72
2	1.1	0.5 to 2	–	–	70	18
3	1.1	–	–	–	70	18
4	1.1	0.5 to 2	–	–	70	5
5	1.1	–	–	–	70	5
6	0.5	–	–	–	45	24
7	0.5	0.5 to 2	–	–	45	24
8	0.5	1	–	–	50	24
9	0.5	1	THF	2 to 12	50	24
10	0.5	1	DMSO	2 to 12	50	24
11	0.5	1	DMF	2 to 12	50	24
12	0.5	1	Anisole	2 to 12	50	24
13	0.5	1	Toluene	2 to 12	50	24

2.3. Synthesis of methacrylated oleic acid via Steglich esterification with HEMA

To enable comparison with the method involving the reaction of glycidyl methacrylate, this work also considered the synthesis of methacrylated oleic acid via Steglich esterification with HEMA. For this purpose, the process described in the literature was considered [10]. Briefly, defined amounts of oleic acid, DMAP and HEMA were mixed in THF in a two-necked flask at room temperature with stirring, and then placed in an ice-water bath purged with N_2 gas. In a separate beaker, DCC was dissolved in the minimum necessary amount of THF and added dropwise to the mixture. The ice-water bath was then removed once the addition of the DCC was complete. After 24 h reaction time, the precipitated urea was filtered off and the THF was removed using a rotary evaporator. The resulting ester was purified by column chromatography using silica gel as the stationary phase and a cyclohexane-EtOAc (95:5, v/v) mixture as the eluent, affording the pure monomer.

2.4. Synthesis of the ATRP macroinitiator mPEG-Br

In order to consider mPEG as a potential hydrophilic block in copolymers involving oleic acid-based hydrophobic blocks, the ATRP macroinitiator mPEG-Br was synthesized using the methodology reported for reactions involving hydroxyl groups and BIBB [32–34]. In brief, a defined amount of mPEG was dispersed in DMF using sonication. Then, triethylamine and DMAP were added to the mPEG dispersion, after which BIBB was added dropwise to the suspension at 0 °C. The reaction was then allowed to proceed at room temperature for 24 h, after which ethanol was used to terminate the esterification. The products were washed with DMF until a colorless liquid phase was achieved, after which the ATRP macroinitiator mPEG-Br was purified with deionized water and dried in a vacuum oven at 40 °C. The resulting ATRP macroinitiator, mPEG-Br, was then used to form block copolymers, considering ATRP processes involving methacrylated oleic acid monomers described in Sections 2.2 and 2.3.

2.5. Synthesis of p(GMA) and p(DMAEMA) homopolymers via RAFT polymerization

The synthesis of the homopolymers p(GMA) and p(DMAEMA) via RAFT polymerization was performed under conditions similar to those reported in the literature [35–38]. These polymerizations were carried out in bulk by dissolving defined amounts of the RAFT agent (CPDT or DBZT) and the initiator (AIBN) in the monomer, after which the mixture was purged with a flow of dry argon for 30 min. The vessel was then sealed, after which polymerization was performed at 60 °C for the selected time. Typical molar ratios used were M/I/RAFT = 7.5/0.02/0.06 (see Table 2 for additional information). The resulting polymers were isolated and purified by successive precipitation in non-solvents (e.g. diethyl ether for p(GMA)) and dialysis using 3.5 k MWCO cellulose bags. For the purification of p(DMAEMA), the method involving the solubilization of the crude polymer in water at pH ~4, followed by increasing the pH to ~12 and the temperature to ~65 °C [39], was adopted here too. The purified RAFT homopolymers were dried at 40 °C in a vacuum oven, after which they were characterized in terms of gravimetric yield, FTIR and SEC analysis.

2.6. Synthesis of p(GMA) and p(DMAEMA) homopolymers via ATRP

The synthesis of the homopolymers p(GMA) and p(DMAEMA) via ATRP polymerization was performed under conditions similar to those reported in the literature [39–45]. These polymerizations were carried out in anisole solvent solution. Briefly, defined amounts of CuBr and ligand (BPY or PMDETA) were dissolved in anisole, then the required amounts of monomer and initiator (EBrP) were added. The mixture was then purged with a flow of dry argon for 30 min. After sealing the vessel, polymerization was performed at 60 °C for the selected time. Typical molar ratios used were M/I/C/L = 2.6/0.1/0.1/0.27 (see Table 2 for additional information). As previously described, the resulting polymers were isolated and purified by successive precipitation in non-solvents and dialysis using 3.5 k MWCO cellulose bags. As above, the purification of p(DMAEMA) also included solubilizing the polymer in water at pH 4, followed by increasing the pH to 12 and the temperature to 65 °C [39]. The purified ATRP homopolymers were dried at 40 °C in a vacuum oven and then characterized in terms of gravimetric yield, FTIR and SEC analysis.

2.7. Synthesis of p(GMA)-b-p(DMAEMA) copolymers via RAFT polymerization

The synthesis of copolymers p(GMA)-*b*-p(DMAEMA) via RAFT polymerization was performed using macro-RAFT agents which synthesis and purification was described in Section 2.5. The p(GMA) or p(DMAEMA) macro-RAFT homopolymers were dissolved in DMSO at the desired concentration in the presence of the required amounts of the correspondent comonomer and AIBN initiator. The mixture was purged with a flow of dry argon for 30 min after which polymerization was performed in the sealed vessel at 60 °C for the selected time. Table 3 provides information about the initial composition of the polymerization mixture. As before, the resulting polymers were isolated and purified by successive precipitation in non-solvents and dialysis. The purified p(GMA)-*b*-p(DMAEMA) copolymers were dried at 40 °C in a vacuum oven, after which they were also characterized in terms of gravimetric yield, FTIR and SEC analysis.

2.8. Synthesis of p(GMA)-b-p(DMAEMA) copolymers via ATRP

The synthesis of the copolymer p(GMA)-*b*-p(DMAEMA) via ATRP polymerization was performed using ATRP macroinitiators, the synthesis and purification of which are described in Section 2.6. These polymerizations were also carried out in a DMSO solvent solution. Defined amounts of CuBr and ligand (BPY or PMDETA) were dissolved in the solvent, and then the required amounts of comonomer and macro ATRP initiator were added. The mixture was purged with a flow of dry argon for 30 min, after which polymerization was performed in a sealed vessel at 60 °C for the selected time. Table 3 provides information about the initial composition of the polymerization mixture. The resulting polymers were isolated and purified by successive precipitation in non-

Table 2
Typical experimental conditions considered for the synthesis of poly(glycidyl methacrylate) and poly(2-(dimethylamino)ethyl methacrylate) homopolymers through the ATRP and RAFT polymerization techniques. All the reactions were performed at 60 °C and the various concentration values provided are expressed in mol/dm^3.

P	Tech.	M		I		C		L		RAFT A.		S	t(h)	Yield (%)
H1	ATRP	GMA	2.6	EBrP	0.10	CuBr	0.1	BPY	0.27	–	–	Anisole	10	77
H2	RAFT	GMA	7.5	AIBN	0.02	–	–	–	–	CPDT	0.06	–	4	56
H3	ATRP	DMAEMA	2.6	EBrP	0.10	CuBr	0.1	BPY	0.27	–	–	Anisole	10	47
H4	RAFT	DMAEMA	6.4	AIBN	0.02	–	–	–	–	CPDT	0.06	–	4	38
H5	RAFT	GMA	7.5	AIBN	0.02	–	–	–	–	DBZT	0.06	–	1	10
H6	ATRP	GMA	2.6	EBrP	0.10	CuBr	0.1	PMDETA	0.1	–	–	Anisole	10	89
H7	ATRP	DMAEMA	2.6	EBrP	0.10	CuBr	0.1	PMDETA	0.1	–	–	Anisole	10	37

Table 3
Typical experimental conditions considered for the synthesis of poly(glycidyl methacrylate)-*b*-poly(2-(dimethylamino)ethyl methacrylate) copolymers through the ATRP and RAFT polymerization techniques. All the reactions were performed at 60 °C and the various concentration values provided are expressed in mol/dm^3, except the correspondent to the used homopolymers that are presented in mg/mL.

P	Tech.	M		I		C		L		RAFT A.		S	t(h)	Mass increase (%)
C1	RAFT	DMAEMA	1.2	AIBN	8×10^{-4}	–	–	–	–	**H2**	24 (mg/mL)	DMSO	5	170
C2	ATRP	DMAEMA	0.8	**H1**	40 (mg/mL)	CuBr	2.1×10^{-3}	BPY	3.5×10^{-3}	–	–	DMSO	5	12
C3	ATRP	DMAEMA	0.4	**H1**	40 (mg/mL)	CuBr	2.1×10^{-3}	BPY	3.5×10^{-3}	–	–	DMSO	5	24

solvents and dialysis. The purified p(GMA)-*b*-p(DMAEMA) copolymers obtained by ATRP were dried at 40 °C in a vacuum oven. They were then characterized in terms of gravimetric yield, FTIR and SEC analysis.

2.9. Incorporation of oleic acid in p(GMA) homopolymers

The incorporation of oleic acid into p(GMA) homopolymers synthesized by ATRP or RAFT polymerization (see Sections 2.5 and 2.6) was carried out in DMSO solution at 60 °C. In brief, the prescribed amounts of oleic acid (OA), p(GMA), the 2MI catalyst and the solvent were mixed and allowed to react for the defined time period. Table 4 provides information about the initial composition of the reaction mixture. The modified p(GMA) product was then isolated and purified by precipitation and dialysis. This was followed by drying at 40 °C in a vacuum oven and characterization in terms of gravimetric yield, FTIR and SEC analysis.

2.10. Incorporation of oleic acid in p(GMA)-b-p(DMAEMA) copolymers

The incorporation of oleic acid into p(GMA)-*b*-p(DMAEMA) copolymers, synthesized by ATRP or RAFT polymerization (see Sections 2.7 and 2.8), was also carried out in DMSO solution at 60 °C, in a manner analogous to that described in Section 2.9 for p(GMA) homopolymers (see Table 5 for information about the initial composition of the reaction mixture).

2.11. One-pot synthesis of p(GMA)-b-p(DMAEMA) copolymers with incorporated OA through ATRP with p(GMA) macroinitiator

The one-pot synthesis of p(GMA)-*b*-p(DMAEMA) copolymers with incorporated OA was performed through the ATRP technique. This process involved the dissolution of the specified amounts of p(GMA) ATRP macroinitiator (see Section 2.6), CuBr, ligand (BPY or PMDETA) and DMAEMA monomer, along with the defined amounts of OA and 2MI catalyst, in DMSO. The mixture was purged with a flow of dry argon for a period of 30 min. This was followed by the promotion of polymerization and reaction of OA with epoxy groups of p(GMA) in a sealed vessel at a temperature of 60 °C for the designated time. Table 5 provides information about the initial composition of the reaction mixture. The resulting polymer product was then isolated and purified by precipitation and dialysis. Subsequent to this, the samples were subjected to drying at a temperature of 40 °C within a vacuum oven. This was followed by characterization in terms of gravimetric yield, FTIR and SEC analysis.

Table 4
Typical experimental conditions considered for the incorporation of oleic acid in poly(glycidyl methacrylate) homopolymers. All the reactions were performed at 60 °C and the various concentration values provided are expressed in mol/dm^3, except the correspondent to the used homo−/copolymers that are presented in mg/mL.

P	Polymer		OA	2-MIZ	S	t (h)	Mass increase (%)
OAI1	**H1**	34.7 (mg/mL)	0.49	4.6×10^{-3}	DMSO	24	40
OAI2	**H2**	34.7 (mg/mL)	0.49	4.6×10^{-3}	DMSO	24	136

2.12. Polymer characterization using SEC/RI/LALS/RALS with DMF solvent

SEC analysis was considered to get information concerning the structure of different DMF soluble homopolymers and copolymers synthesized in this research. The used SEC apparatus is composed of a Viscotek GPCmax VE 2001 pumping system with Refractive Index (RI), Low Angle Light Scattering (LALS) and Right Angle Light Scattering (RALS) detection. Polymers were fractionated in a train of 2 Phenogel columns: 1) 500 Å (molecular weight 1 k to 15 k) + 2) 1000 Å (molecular weight 1 k to 75 k) with dimensions L × D = 300 mm × 7.5 mm. DMF with 20 mM LiBr was used as eluent and the measurements were performed at 50 °C and Q = 1 mL/min.

2.13. Polymer characterization using SEC/RI/MALLS with chloroform solvent

Chloroform soluble homopolymers and copolymers were analyzed using a different SEC apparatus that is composed of a Polymer Laboratories PL-GPC-50 integrated SEC system with differential refractometer working at 950 ± 30 nm, attached to a Wyatt Technology DAWN8$^+$ HELEOS 658 nm MALLS detector. The polymer samples were fractionated by molecular size using a train of 3 GPC columns PLgel (300 mm × 7.5 mm) with nominal particle size 10 μm and pore type MIXEDB-LS, maintained at constant temperature of 30 °C and using chloroform as the eluent at a flow rate of 1 mL/min.

2.14. FTIR analysis of the polymers

Purified and dried products were characterized through FT-IR spectroscopy with a Perkin Elmer, model Spectrum Two™, instrument. These analyses were directly performed in ATR mode or, when needed, polymers were mixed with KBr and pressed into pellets in order to collect the correspondent IR spectra.

2.15. Encapsulation and release of oleanolic acid with the synthesized amphiphilic copolymers

Block amphiphilic copolymers were first dissolved in THF in the presence of oleanolic acid and afterwards the solvent composition was dropwise changed up to reach THF/water 50/50. The final solution was dialyzed against water in a cellulose bag membrane (3.5 k molecular weight cut off). The estimation of the encapsulated oleanolic acid was obtained through HPLC-DAD analysis of the liquid phase after filtration, considering both the THF/water 50/50 system and the final aqueous dispersion. Final aqueous dispersions were subjected to the analysis of oleanolic release by dropping in water with defined values of pH and temperature. Released oleanolic acid was also quantified through HPLC-DAD analysis of the liquid phase after filtration. The suitability of block amphiphilic copolymers for the formation of aggregates and encapsulation of hydrophobic compounds was also assessed using Nile Red and following visually the color change along the self-assembly process. Encapsulation of oleanolic acid in a solid dispersion was also performed using p(GMA-OA)-*b*-p(DMAEMA) materials acting as a polymeric carrier

Table 5
Typical experimental conditions considered for the incorporation of oleic acid in poly(glycidyl methacrylate)-*b*-poly(2-(dimethylamino)ethyl methacrylate) copolymers. All the reactions were performed at 60 °C and the various concentration values provided are expressed in mol/dm^3, except the correspondent to the used homo−/copolymers that are presented in mg/mL.

P	Polymer		OA	2-MIZ	M		I		C		L		RAFT A.		S	t (h)	Mass increase (%)
OAP1	**C1**	34.7 (mg/mL)	0.49	4.6×10^{-3}	–	–	–	–	–	–	–	–	–	–	DMSO	24	280
OAP2	**C2**	34.7 (mg/mL)	0.49	4.6×10^{-3}	–	–	–	–	–	–	–	–	–	–	DMSO	24	240
OAP3	**C3**	34.7 (mg/mL)	0.49	4.6×10^{-3}	–	–	–	–	–	–	–	–	–	–	DMSO	24	177
OAP4	**H1**	34.7 (mg/mL)	0.49	4.6×10^{-3}	DMAEMA	0.7	–	–	CuBr	2.1×10^{-3}	BPY	3.4×10^{-3}	–	–	DMSO	24	255

and a solvent evaporation method with THF.

2.16. SEM and TEM analysis

Dried polymer particles were analyzed by scanning electron microscopy (SEM) with an FEI Quanta 650 FEG scanning electron microscope under a high vacuum. Secondary electrons were detected by an Everhardt Thornley SED (secondary electron detector). The images were acquired at 10 kV, spot size 3 and with a working distance of 10 mm. The samples were sputtered with gold, using the following setup: sputtering current = 30 mA and duration = 30 s. Stable aqueous dispersions of aggregates encapsulating oleanolic acid were analyzed by TEM with a probe-corrected FEI Titan G2 80–200 kV ChemiSTEM set-up. Such aggregates were formed by self-assembling of the synthesized p(GMA-OA)-*b*-p(DMAEMA) copolymers. These SEM and TEM analyses were performed at the national Iberian Nanotechnology Laboratory (INL), Braga, Portugal.

2.17. HPLC-DAD analysis for quantification of encapsulation and release of oleanolic acid with the synthesized amphiphilic copolymers

An HPLC system (KNAUER) consisting of a gradient pump (P6.1 L) equipped with a degasser, an autosampler (6.1 L), a column thermostat (CT2.1), and a DAD (6.1 L) was used in this research. ClarityChrom was the software allowing the control of the HPLC-DAD (High-Performance Liquid Chromatography with Diode Array Detector) system. The chromatographic analysis was performed using an Ascentis C18 (SUPELCO) column with a particle size of 5 μm and dimensions 25 cm × 4.6 mm. An isocratic analysis was performed, using ACN/water 85/15 with 0.05 % formic acid as eluent, for 25 min at $T = 25$ °C.

2.18. UV/Vis spectroscopy and HPLC-DAD for monitoring purification processes

A spectrophotometer P9 Double Beam UV–Visible, VWR, was used for fast assessment of cleaning and purification steps described above. The HPLC-DAD system outlined in Section 2.17 was also used to assess the purification processes by analyzing the liquid phases involved, as well as to quantify GMA conversion in the different reaction routes detailed above (liquid phase analysis).

3. Results and discussion

The synthesis of methacrylated derivatives of natural fatty acids via the catalytic reaction between epoxy and carboxylic acid groups is a widely considered topic in current research and industrial applications. Among compounds with vinyl and epoxy reactive groups, glycidyl methacrylate is often preferred due to its simplicity of preparation from methacrylic acid and glycidol, and its peculiar reactivity enables it to undergo many polymerization reactions, as well as post-polymerization modification mechanisms. This approach is used to prepare vinyl monomers that incorporate oleic acid, among others, with the aim of developing more sustainable coatings and adhesives [2–7]. Interestingly, the unique reactivity and post-polymerization modification possibilities of GMA have also been explored in the preparation of advanced block copolymers, namely using controlled radical polymerization techniques [17,19,20,35–37]. This research combines the two working lines to synthesize hybrid synthetic-natural block copolymers comprising a hydrophobic block resulting from the reaction between oleic acid and the epoxy groups of GMA, and a hydrophilic part based on p(DMAEMA). To this end, various reaction routes are assessed here, including the methacrylation of oleic acid and post-polymerization modifications, with the aim of minimizing side reactions that could have a detrimental effect on the properties of the desired amphiphilic block copolymers.

3.1. Experiments with methacrylated oleic acid monomer (MOA)

Table 1 provides an overview of the various operating conditions considered in this study for synthesizing methacrylated oleic acid monomer (MOA) through a reaction with glycidyl methacrylate. The synthesis described by runs 1 to 5 follows operating conditions like those reported in the literature for the reaction between OA and GMA, with the aim of preparing monomers for use in a subsequent free radical process for applications in the coating industry or for polymer networks [4,7–9]. FTIR analysis of the products shows that the epoxy groups of GMA are consumed in these reactions involving the methacrylation of oleic acid (the disappearance of the 910 cm^{-1} peak was followed), with total depletion observed in Run 1 and partial conversion in the others. The products of runs 1 to 5 were not fully soluble in ethanol, methanol, acetonitrile, DMF, DMSO, THF or chloroform at concentrations of 1 mg/mL or lower and temperatures up to 70 °C. The MOA products were also insoluble in the DMAEMA monomer, which was intended for use as the second building block in the production of the desired amphiphilic copolymers. These insolubility observations are consistent with the formation of branched species due to secondary reactions as depicted in Fig. 1 and reported in the literature [9,21]. However, it was possible to carry out their free radical polymerization with styrene at 70 °C using an AIBN initiator, as demonstrated by the analysis of the products (see Fig. S3 in Supplementary Information), in accordance with the previously described procedure [9]. This confirms that using these synthesis recipes to generate MOA monomers is an effective approach for the subsequent production of branched/cross-linked materials. The ATRP and RAFT homopolymerization of the soluble part of the MOA monomers obtained in runs 1 to 5 produced gel-like products that were also unsuitable for the intended block copolymer synthesis.

Runs 6 to 13 in Table 1 were designed to minimize secondary reactions leading to branching/crosslinking (see Fig. 1). To this end, a molar excess of OA compared to GMA was employed, along with the absence of, or an alternative to, the catalyst (KOH attempted in these runs, as reported in Ref. [21]), and dilution with a solvent or decreased temperature. Homogeneous solutions were observed after the reaction

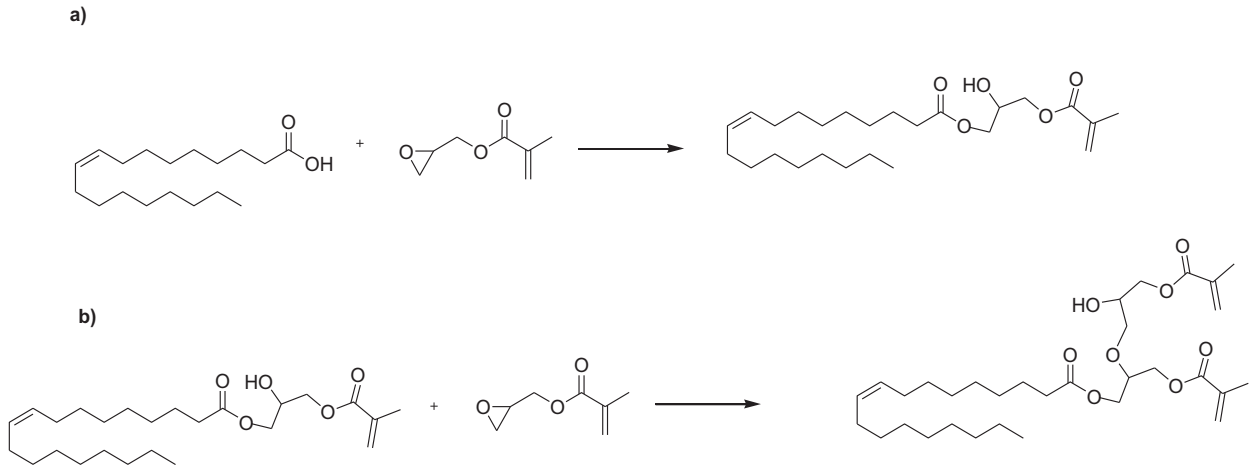

Fig. 1. a) A schematic representation of the formation of methacrylated oleic acid through a reaction with glycidyl methacrylate. b) A secondary reaction involving epoxides and the hydroxyl groups formed in the main route, which leads to the formation of multifunctional species. These species can react in later stages to form high-molecular-weight branched/crosslinked molecules.

in the specified solvents, and the conversion of GMA was estimated to be around 50 % by HPLC-DAD. FTIR analysis of the solutions also demonstrates incomplete epoxide conversion. These results indicate the formation of MOA and the limitation of branching to an acceptable level. However, difficulties were encountered in product separation, particularly regarding the removal of unreacted OA (a saponification process was attempted) and the isolation of MOA resulted in a very low final yield (<10 %). Note that laborious procedures are also needed to make the separation and purification of methacrylated OA when alternative methods, such as the esterification with HEMA, as described in Section 2.3, are considered. A final yield of around 70 % was observed when this approach was adopted. The use of the MOA monomers obtained via OA reaction with GMA or Steglich esterification with HEMA for block copolymers generation using ATRP and the *m*PEG-Br macroinitiator (see Section 2.4) was demonstrated to be possible (see Figs. S4 and S5 in SI) but at very low conversion yield (<5 %). Furthermore, attempts to generate homopolymers via ATRP/RAFT using MOA monomers produced via OA/GMA reaction or OA/HEMA esterification also resulted in very low polymerization yields (<10 %), hindering the subsequent step of generating amphiphilic block copolymers with DMAEMA. This is likely the result of the reactivity of the MOA monomers being too low within the ATRP/RAFT processes. Difficulties observed with the simultaneous dissolution of the MOA monomers and RAFT/ATRP components also contributes to this shortcoming. Overall, the production of the intended p(GMA-OA)-*b*-p(DMAEMA) copolymers using MOA monomer was found to be challenging in terms of scalability.

3.2. Experiments with post-polymerization modification of GMA moieties

Given the shortcomings described above in the synthesis of MOA monomers and their potential subsequent use in producing ATRP/RAFT amphiphilic block copolymers, alternative post-polymerization routes with GMA modification were explored. Interestingly, these results demonstrate the potential to control the branching degree in the OA/GMA reaction, particularly when excess OA and diluted conditions are considered. Therefore, post-polymerization modification of homo and copolymers containing GMA moieties was adopted under these reaction conditions.

Figs. 2 to 6 depict the various reaction pathways involved in this post-polymerization modification approach. Fig. 2 shows the formation of the p(GMA-OA) homopolymer through the transformation of the p(GMA) polymer with OA. Fig. 3 illustrates the production of the p(GMA-OA)-*b*-p(DMAEMA) copolymer using pre-formed p(GMA-OA) in ATRP or RAFT processes. Fig. 4 shows the synthesis of the block copolymer p(GMA)-*b*-p(DMAEMA) by RAFT or ATRP, while Fig. 5 shows its transformation into a p(GMA-OA)-*b*-p(DMAEMA) copolymer via reaction

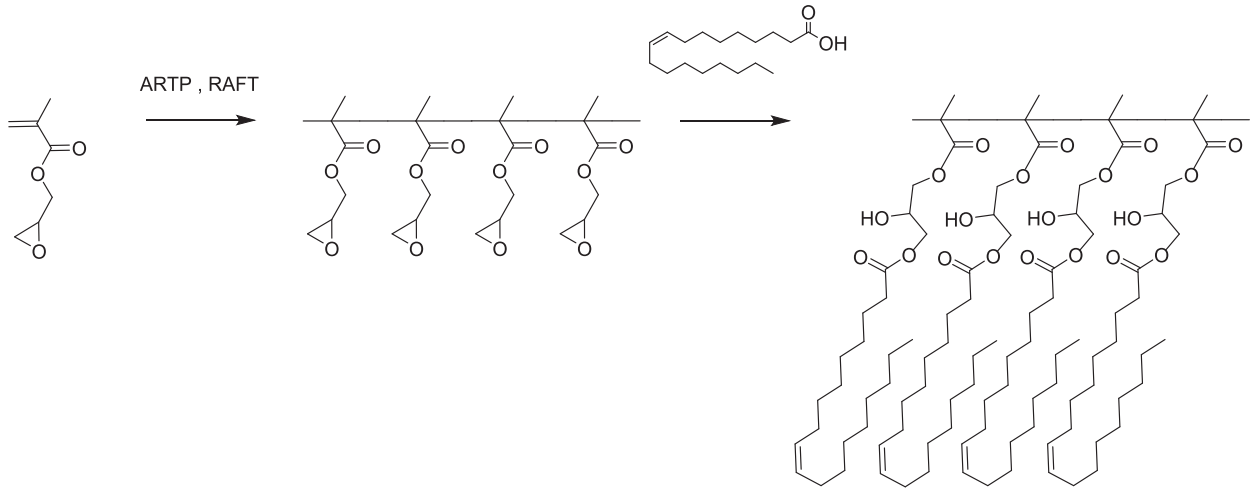

Fig. 2. A schematic representation of the synthesis of p(GMA) homopolymers via ATRP or RAFT polymerization. It also shows the post-polymerization modification of the p(GMA) homopolymers through the reaction of OA with the epoxides in the repeating units, leading to the formation of a p(GMA-OA) homopolymer.

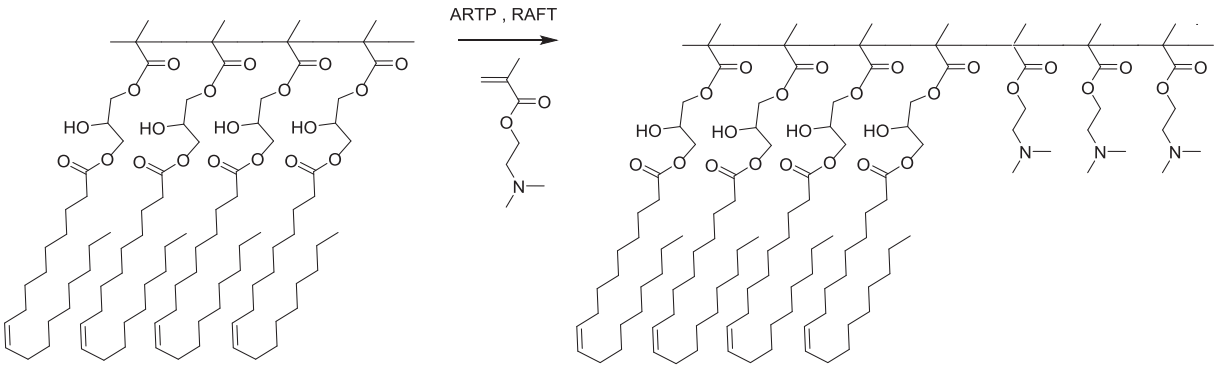

Fig. 3. A schematic representation of the synthesis of a p(GMA-OA)-*b*-p(DMAEMA) copolymer via ATRP or RAFT polymerization. These polymerizations use the previously synthesized p(GMA-OA) homopolymer (Fig. 2) as the macro-initiator or macro-RAFT agent, respectively.

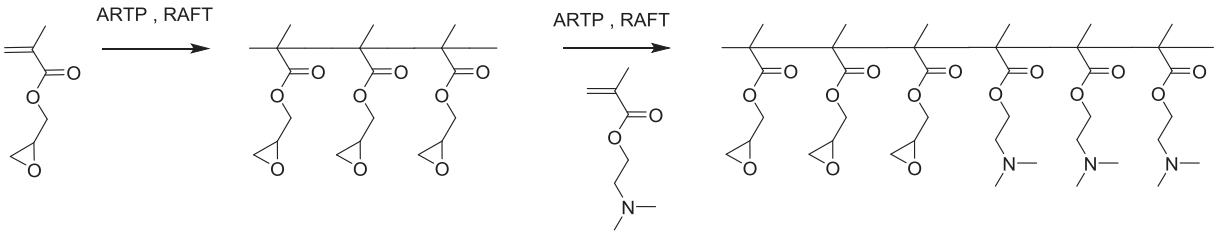

Fig. 4. A schematic representation of the synthesis of the block copolymer p(GMA)-*b*-p(DMAEMA), using the corresponding previously synthesized p(GMA) homopolymers as the macro-initiator or macro-RAFT agent.

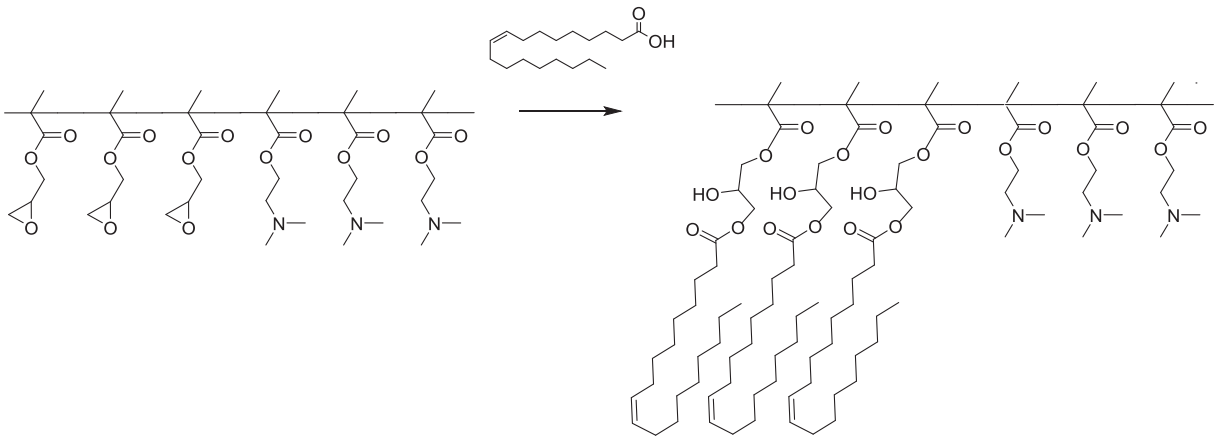

Fig. 5. A schematic representation of the synthesis of a p(GMA-OA)-*b*-p(DMAEMA) copolymer through the post-polymerization modification of a p(GMA)-*b*-p(DMAEMA) copolymer. This route considers the reaction of OA with the epoxides in the repeating units of p(GMA)-*b*-p(DMAEMA) for the formation of p(GMA-OA)-*b*-p(DMAEMA).

with OA. Finally, Fig. 6 shows a diagram of the one-pot synthesis of a p(GMA-OA)-*b*-p(DMAEMA) copolymer, which involves the simultaneous post-polymerization modification of a p(GMA) homopolymer and DMAEMA polymerization.

Table 2 provides information on the experimental conditions for synthesizing p(GMA) and p(DMAEMA) homopolymers using ATRP and RAFT polymerization techniques. This is the first step in any post-polymerization transformation route aimed at producing p(GMA-OA)-*b*-p(DMAEMA) amphiphilic block copolymers. These recipes follow general principles reported for the ATRP and RAFT homopolymerization of GMA or DMAEMA [35–45]. Indeed, the synthesis of various types of homo- and block copolymers or grafted materials, including the GMA and DMAEMA monomers, based on ATRP and RAFT polymerization techniques, has been reported in recent years [35–45]. These studies explore the versatility of GMA moieties for subsequent functionalization [40,41] and the excellent performance of DMAEMA materials for adsorption [38] and gene delivery due to their biocompatibility [45], among other applications. The reaction time was adjusted to prevent the formation of bulky homopolymers that would hinder their solubilization in subsequent steps, with the aim of using them as macroinitiators or macro-RAFT agents for block copolymers formation. The yield shown in Table 2 was calculated by dividing the mass of the isolated polymer by the initial mass of the monomer.

The recipes in Tables 3 to 5 describe the various experimental conditions that were investigated in this study to produce p(GMA)-*b*-p(DMAEMA) and p(GMA-OA)-*b*-p(DMAEMA) copolymers. In this context, it is particularly relevant that DMSO was selected as the solvent in an attempt to reduce the incidence of branching reactions due to the high reactivity of the oxirane ring and the derived hydroxyl group [1]. Indeed, it has been reported that using DMSO as a solvent result in

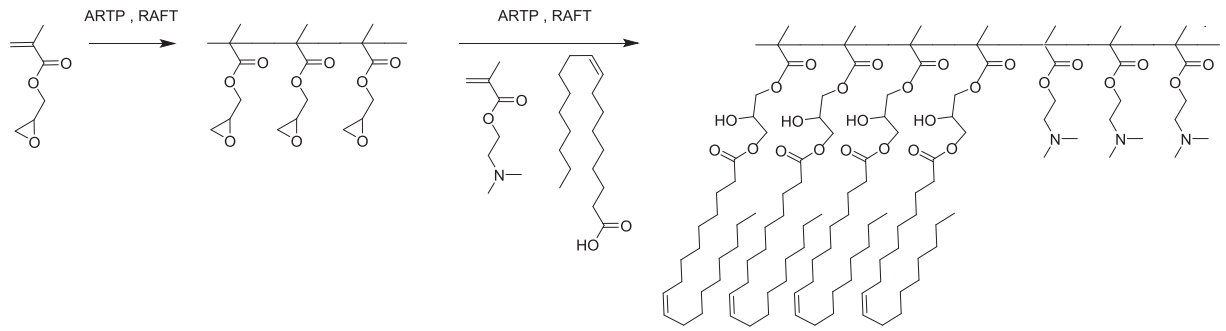

Fig. 6. A schematic representation of the one-pot synthesis of a p(GMA-OA)-*b*-p(DMAEMA) copolymer via the simultaneous post-polymerization modification of a p (GMA) homopolymer and DMAEMA polymerization. These ATRP and RAFT processes utilize the previously synthesized p(GMA) homopolymers as the macro-initiator and macro-RAFT agent, respectively, while the epoxy groups in their moieties undergo a reaction with OA.

polymers maintaining linearity when different nucleophilic agents are used (e.g. secondary amines, thiols, aromatic alcohols and the azide anion) in the post-polymerization treatment of p(GMA) [1]. The proposed treatment conditions in DMSO require a short reaction time to avoid the formation of micro- and macro-gels, which are often observed with alternative, longer-time p(GMA) modification processes that also aim for full conversion of the epoxy groups [1]. These outcomes were adapted for the reaction between oleic acid and the epoxide groups in p (GMA) homopolymer or p(GMA)-*b*-p(DMAEMA) copolymer moieties, as detailed in Tables 4 and 5. For compatibility purposes, DMSO was also selected as the solvent for the synthesis of p(GMA)-*b*-p(DMAEMA) copolymers, as described in Table 3. The reaction time was optimized to achieve total conversion of the epoxide groups (see FTIR characterization below), and the recipes for incorporating oleic acid were designed to use a stoichiometric excess of OA compared to the epoxides to try the minimization of secondary reactions involving the oxirane ring. The

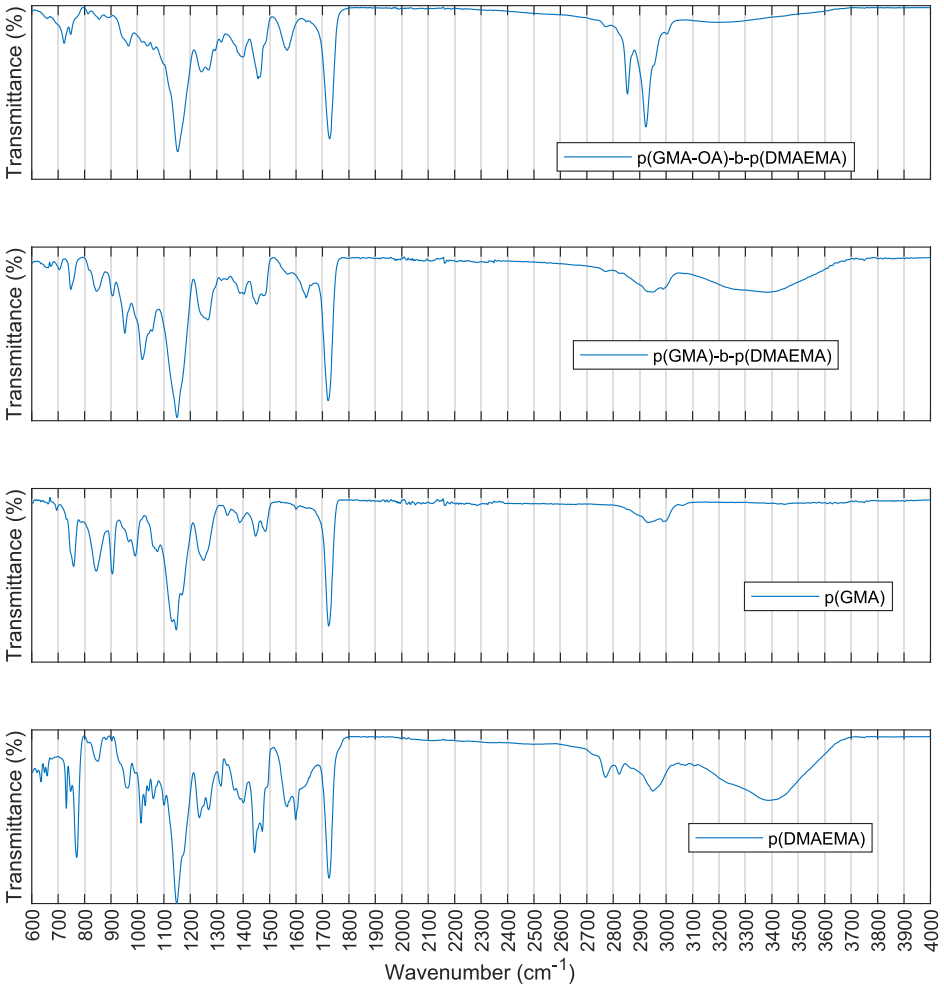

Fig. 7. FTIR analysis of a product p(GMA-OA)-*b*-p(DMAEMA), a block copolymer p(GMA)-*b*-p(DMAEMA) and related homopolymers p(GMA) and p(DMAEMA). Specific assignment at 910 cm^{-1} is observable in the p(GMA) homopolymer and in the p(GMA)-*b*-p(DMAEMA) copolymer but not in the product p(GMA-OA)-*b*-p (DMAEMA), indicating the reaction of the epoxide moieties of the p(GMA) block with oleic acid. On the other hand, specific assignments at 2770 cm^{-1} ($-N(CH3)_2$) groups, are also discernible in both copolymers and in the p(DMAEMA) homopolymer. The increased prominence of the band in the 2800–3000 cm^{-1} region and the enhanced vibrational assignment at 1466 cm^{-1} both indicate successful oleic acid incorporation into the final p(GMA-OA)-*b*-p(DMAEMA) product.

mass increase values reported in Tables 3 to 5 are calculated by comparing the mass recovered for the final product with the initial mass of the polymer used in the reaction, $100 \times (m_{product} - m_{polymer})/m_{polymer}$.

3.3. FTIR analysis

FTIR analysis was performed to evaluate the incorporation of different building units into various homopolymers and copolymers, including p(GMA), p(DMAEMA), p(GMA)-*b*-p(DMAEMA), and p(GMA-OA)-*b*-p(DMAEMA). Fig. 7 shows the results of the FTIR analysis of representative products, and further related information is provided in the Supplementary Information (SI). The specific assignment at 910 cm^{-1}, corresponding to the stretching vibration of the epoxy ring, is observed in p(GMA) and p(GMA)-*b*-p(DMAEMA), but not in p(GMA-OA)-*b*-p(DMAEMA). This indicates the successful formation of p(GMA)-*b*-p(DMAEMA), and the latter reaction of the contained epoxy groups with oleic acid. Note also that the expected specific vibrational assignments due to the DMAEMA moiety, corresponding to the $–N(CH_3)_2$ groups at around 2770 cm^{-1}, are observed in p(DMAEMA), as well as in p(GMA)-*b*-p(DMAEMA). Combined with the 910 cm^{-1} assignment, this demonstrates the presence of both the GMA and DMAEMA moieties in the copolymer. Notably, in the p(GMA-OA)-*b*-p(DMAEMA) product, the increased prominence of the band in the 2800–3000 cm^{-1} region (CH_2 and CH_3 stretching) and the enhanced vibrational assignment at 1466 cm^{-1} (OH in plane bending) both indicate successful oleic acid incorporation into the final p(GMA-OA)-*b*-p(DMAEMA) product.

Figs. S6–S12 in the SI provide additional evidences obtained by FTIR for the achievement of the compositional features designed for intermediate and final materials described in Tables 2 to 5.

3.4. GPC analysis

GPC analysis was considered in order to obtain information regarding the chain length distribution of the intermediates and final products involved in the synthesis of the target p(GMA-OA)-*b*-p(DMAEMA) copolymers. To this end, two alternative GPC systems running with dimethylformamide and chloroform were employed, as outlined in the experimental section. It should be noted that the GPC analysis of amphiphilic copolymers is generally problematic due to the significant solubility limitations of the materials in conventional GPC solvents, as well as the multiple interaction effects between the copolymer's different domains (e.g., hydrophilic/hydrophobic segments) and the sorbent particles in the GPC columns. Therefore, the GPC analysis of these block copolymers often provides information about an apparent chain length distribution rather than an absolute one. Nevertheless, this information is still useful because it allows different block amphiphilic copolymers of the same kind to be compared.

Figs. 8 to 11 and Table 6 provide an overview of the GPC analysis results for the characterization of various homopolymers and copolymers involved in this research. The ATRP and RAFT synthesized homopolymers of p(GMA) and p(DMAEMA), products H1 to H7 in Table 2, were analyzed in DMF due to significant solubility limitations in chloroform. Fig. 8 presents the SEC traces observed for the p(GMA) homopolymers synthesized by ATRP and RAFT under conditions H1 and H2. The polydispersity index is estimated to be around 1.3 for both the ATRP (H1) and RAFT (H2) products, with weight-average molecular weights of 2.6×10^4 and 1.8×10^4, respectively. Both homopolymers are suitable for further processing with the introduction of the p(DMAEMA) segment. Furthermore, these p(GMA) homopolymers exhibited a simple isolation process and a reasonable yield was achieved (77 % and 56 % for H1 and H2, respectively, as detailed in Table 2). Fig. 9, on the other hand, presents the SEC traces observed for the p(DMAEMA) homopolymers synthesized by ATRP and RAFT under conditions H3 and H4. The polydispersity is estimated to be around 1.5 and 1.2 for these products, and the molecular weight was measured to be in a lower range, compared with the p(GMA) homopolymers (see Table 6). A more laborious isolation process was needed with the p(DMAEMA) homopolymers (see Experimental section) and lower yields were measured (47 % and 38 % for H3 and H4, respectively). Product H5 was investigated as an alternative to RAFT-synthesized p(GMA), using DBZT trithiocarbonate as the chain transfer agent. However, poor solubility in DMF was observed, indicating the possible formation of a high-molecular-weight polymer due to inefficient RAFT polymerization. GPC analysis of the soluble fraction (see Fig. S13 in the Supplementary Information and Table 6) suggests that control of RAFT polymerization of GMA with DBZT is lower than with the CPDT chain transfer agent. H6 and H7 in Table 2 were examined as possible alternative routes in ATRP for the synthesis of p(GMA) and p(DMAEMA) homopolymers, with PMDETA acting as the ligand instead of BPY. However, under the working conditions used, these products also exhibited limited solubility in DMF and poor control of the polymers' molecular architecture was observed (see Fig. S13 and Table 6).

In light of the aforementioned results concerning the p(GMA)

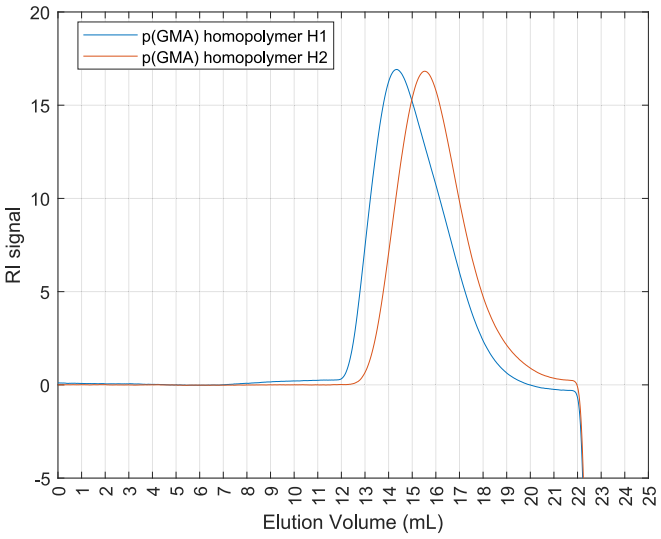

Fig. 8. SEC/RI traces observed for different p(GMA) homopolymers synthesized by ATRP and RAFT according to the conditions **H1** and **H2** in Table 2. SEC analysis performed with DMF solvent at 50 °C and flowrate 1 mL/min.

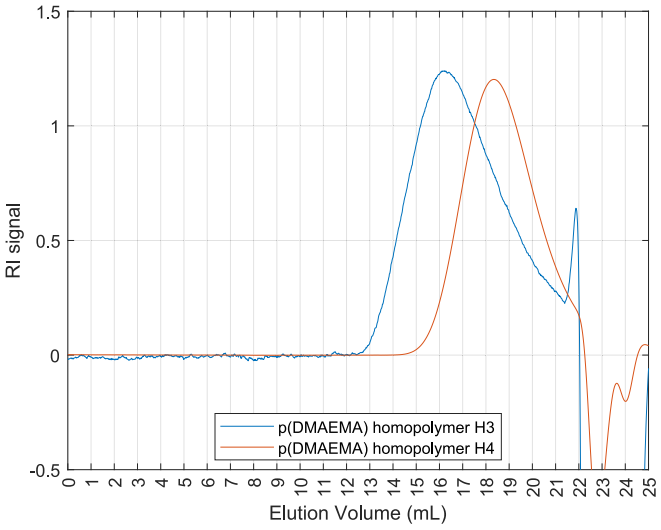

Fig. 9. SEC/RI traces observed for different p(DMAEMA) homopolymers synthesized by ATRP and RAFT according to the conditions **H3** and **H4** in Table 2. SEC analysis performed with DMF solvent at 50 °C and flowrate 1 mL/min.

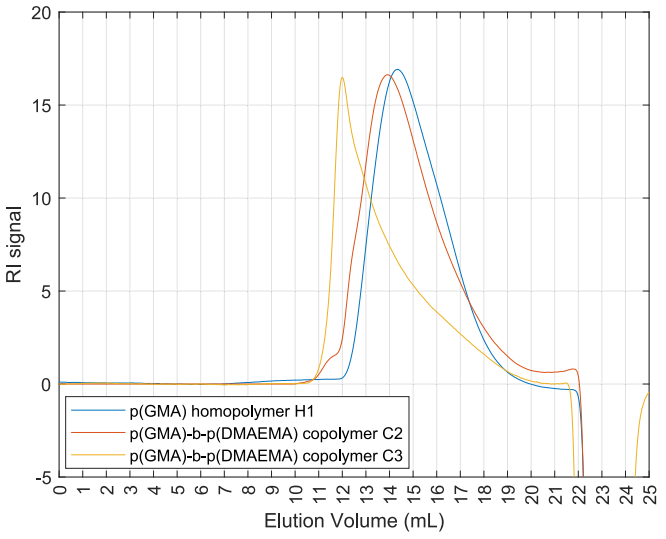

Fig. 10. SEC/RI trace observed for the **H1** p(GMA) homopolymer synthesized by ATRP and the related p(GMA)-*b*-p(DMAEMA) homopolymers synthesized by ATRP according to the conditions **C2** and **C3** in Table 3. SEC analysis performed with DMF solvent at 50 °C and flowrate 1 mL/min.

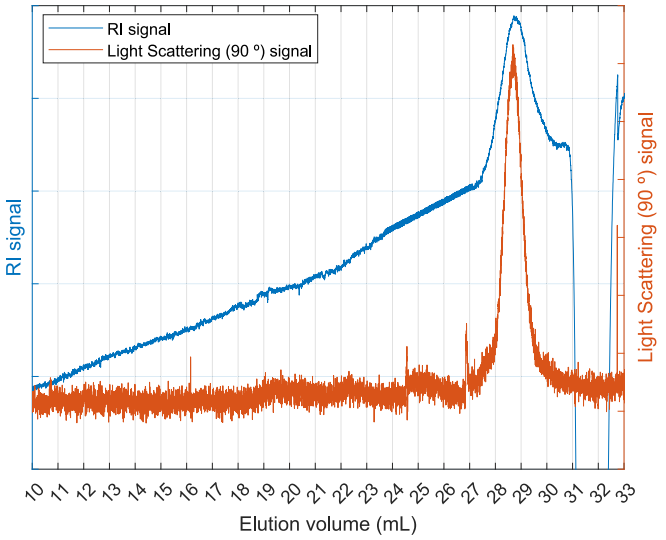

Fig. 11. SEC/RI trace observed for the **OAP4** p(GMA-OA)-*b*-p(DMAEMA) copolymer synthesized according to the conditions in Table 5. SEC analysis performed with chloroform solvent at 30 °C and flowrate 1 mL/min. The refractive index (RI) signal and light scattering (LS) signal at the 90°detector are here presented.

homopolymers obtained via ATRP and RAFT polymerization, the H1 and H2 products were identified as the primary building blocks for synthesizing the desired p(GMA)-*b*-p(DMAEMA) copolymers, as outlined in Table 3 and illustrated in Fig. 4. The p(GMA) homopolymers were employed as either a macroinitiator (H1) in the ATRP process or a macro-chain transfer agent (H2) in the RAFT mechanism, with the objective of building the p(DMAEMA) block within the desired p(GMA)-*b*-p(DMAEMA) copolymers. The resulting copolymers C1, C2 and C3 (Table 3) were also analyzed by GPC (see also the FTIR characterization previously detailed) and the results for C2 and C3 (ATRP synthesized) are presented in Fig. 10 and Table 6. Fig. 10 shows the SEC traces for C2 and C3 in DMF (solubilization of the copolymers in chloroform was not possible) and the corresponding analysis for the H1 - p(GMA) homopolymer is also shown. Compared to the starting p(GMA) homopolymer,

Table 6
Overview of the results obtained with the GPC analysis of various homopolymers and copolymers involved in this research.

Polymer	Product	Polymerization technique	$\overline{M}_n$	$\overline{M}_w$	PDI
p(GMA)	**H1**	ATRP	2.0×10^4	2.6×10^4	1.3
p(GMA)	**H2**	RAFT	1.4×10^4	1.8×10^4	1.3
p(DMAEMA)	**H3**	ATRP	9.1×10^3	1.4×10^4	1.5
p(DMAEMA)	**H4**	RAFT	5.7×10^3	7.1×10^3	1.2
p(GMA)	**H5***	RAFT	4.2×10^4	6.1×10^4	1.5
p(GMA)	**H6***	ATRP	8.4×10^3	1.4×10^4	1.6
p(DMAEMA)	**H7***	ATRP	9.0×10^3	3.1×10^4	3.5
p(GMA)-*b*-p (DMAEMA)	**C2**	ATRP	2.7×10^4	4.3×10^4	1.6
p(GMA)-*b*-p (DMAEMA)	**C3**	ATRP	1.9×10^4	2.9×10^4	1.6
p(GMA-OA)-*b*-p (DMAEMA)	**OAP4***	ATRP	1.5×10^4	2.5×10^4	1.7

* A limited solubility was observed for H5, H6 and H7 in DMF while the analysis for OAP4 was performed in chloroform.

a shift to the high molecular weight region is observed for the copolymers, demonstrating the modification of the starting p(GMA) with the introduction of the p(DMAEMA) block (see also the average properties of C2 and C3 compared to H1 in Table 6 as well as the FTIR results in Figs. S9 and S10). In contrast to C2 and C3, the C1 copolymer obtained from H2 through RAFT polymerization could not be properly solubilized for GPC characterization, indicating lower control of the RAFT process involved in the formation of the p(GMA)-*b*-p(DMAEMA) copolymer, with possible formation of free p(DMAEMA) polymer via uncontrolled radical reaction, as previously examined with the corresponding FTIR analysis (Fig. S8). Note also the significant increase in mass observed with C1 compared to C2 and C3, which is also consistent with the formation of free p(DMAEMA) via FRP during the RAFT process.

The incorporation of oleic acid into the p(GMA) homopolymers H1 and H2 was considered as a possible intermediate step in the formation of the final p(GMA-OA)-*b*-p(DMAEMA) copolymers. This process is detailed in Table 4 and illustrated in Fig. 2 for the formation of the p(GMA-OA) block. FTIR analysis demonstrates successful oleic acid incorporation in H1 and H2 to form OAI1 and OAI2, respectively (see Fig. S11). However, limited solubility was observed in DMF, chloroform and other common solvents with products OAI1 and OAI2. This prevented GPC characterization of these products by SEC, as well as proceeding easily to the next step of incorporating the p(DMAEMA) block into the p(GMA-OA) products.

Table 5 shows the synthesis conditions used in this study to produce the desired p(GMA-OA)-*b*-p(DMAEMA) copolymers. Products OAP1 to OAP3 were obtained by incorporating oleic acid into C1 to C3 p(GMA)-*b*-p(DMAEMA) copolymers, as illustrated in Fig. 5. Product OAP4 is the result of a process involving the simultaneous attachment of the p(DMAEMA) block to the starting p(GMA) homopolymer (H1) via ATRP, alongside the incorporation of OA into the same p(GMA) segment. This process is depicted in Fig. 6. Among the OAP1 to OAP4 p(GMA-OA)-*b*-p(DMAEMA) copolymers only OAP4 could be partially solubilized in chloroform for GPC analysis which result is presented in Fig. 11. The recorded RI and light scattering signals confirm the presence of a polymer population with an apparent $\overline{M}_w$ =2.5 × 10^4 and PDI =1.7. Note also the FTIR results confirming the presence of a p(DMAEMA) block in OAP4 and the incorporation of OA, similarly to products OAP1 to OAP4 (see Fig. S12). A process similar to that considered for OAP4,

which used RAFT polymerization, was found to have low polymerization efficiency.

Considering the molecular weight of the repeating unit in p(GMA) and that of OA, an ideal stoichiometric reaction between the epoxy groups and the hydroxyl groups in the fatty acid would result in a limiting value for mass increase of close to 198 % (mass increase percentage defined as $100 \times \left(m_{p(GMA-OA)} - m_{pGMA}\right)/m_{pGMA}$). In order to decrease the side reactions of the epoxide groups, the reactions for the incorporation of OA were performed with a stoichiometric excess of this component close to 3. Some of the final products exceeded the 198 % limit (see Table 5), which is likely due to the difficulty of removing unreacted OA from the polymer matrix. Taking more stringent cleaning steps should overcome this issue, but the presence of oleanolic acid in the final products does not limit the application of the p(GMA-OA)-*b*-p(DMAEMA) copolymers for the encapsulation and release of hydrophobic molecules, as described below. In Table 7 is presented a comparison of the different synthetic approaches used here for the incorporation of OA in amphiphilic block copolymers through the reaction with GMA.

3.5. SEM and TEM analysis

The developed p(GMA-OA)-*b*-p(DMAEMA) copolymers were applied in this work for the encapsulation of oleanolic acid due to their amphiphilicity. Both the formation of solid dispersions and microemulsions/nanodispersions with these materials were scrutinized, as detailed in the section below. SEM and TEM analyses were performed to gain information on the morphological features of these solid-state and liquid dispersions, as presented in Figs. 12 and 13.

The solid particles shown in Fig. 12 are the result of dispersing the p(GMA-OA)-*b*-p(DMAEMA) copolymers in THF in the presence of oleanolic acid. This is followed by evaporating the solvent in order to create a polymeric carrier. These images reveal amorphous materials that are dispersed in size and form agglomerates with dimensions of up to around 1 mm. At microscale, nucleus of agglomeration can be observed, with sizes ranging from approximately 1 μm (see Fig. 12(6)). Note that these dry particles undergo a significant morphological change when in contact with a solvent, specifically an aqueous mixture. The hydrophilic p(DMAEMA) domain can be solvated by water, resulting in significant swelling of these particles, particularly in acidic environments, due to the ionization of the tertiary amine groups in the DMAEMA polymer moieties. The details of these features are provided below in the context of delivering oleanolic acid using the polymeric carrier p(GMA-OA)-*b*-p(DMAEMA).

The TEM images presented in Fig. 13 correspond to the liquid dispersions that were prepared using p(GMA-OA)-*b*-p(DMAEMA) for the encapsulation of oleanolic acid. The copolymers were first dispersed with oleanolic acid in THF, and then transferred to an aqueous solvent via dialysis in a cellulose bag. Notably, Fig. 13(1) and (2) show well defined spherical particles with size 20 to ~100 nm with an external shell with thickness around 5 to 8 nm that were achieved using the p(GMA-OA)-*b*-p(DMAEMA) amphiphilic copolymer OAP1. These results demonstrate the self-assembly ability of the developed amphiphilic materials in the transition from THF to water, forming a hydrophilic corona based on the p(DMAEMA) block and a hydrophobic p(GMA-OA) core, which can encapsulate oleanolic acid.

Fig. 13(3-4) also shows the nanodispersion achieved using the p(GMA-OA)-*b*-p(DMAEMA) amphiphilic copolymers, containing spherical particle aggregates dispersed over a range of sizes up to ~200 nm.

Interestingly, core/shell nanoparticles with a size of up to 500 nm were observed when the self-assembled aqueous dispersions were generated using a p(GMA-OA)-*b*-p(DMAEMA) material synthesized by ATRP with the simultaneous incorporation of OA (OAP4), as shown in Fig. 13. These results demonstrate that the synthesis conditions influence the molecular architecture of amphiphilic copolymers, which in turn affects the morphology of self-assembled nanostructures. See [26] for more information on the relationship between the size of hydrophobic and hydrophilic blocks in copolymers and the size distribution of aggregates.

Overall, the TEM results presented in Fig. 13 demonstrate that the proposed synthesis routes lead to the formation of amphiphilic copolymers of the type p(GMA-OA)-*b*-p(DMAEMA), which are capable of self-assembling in an aqueous environment to form nano-carriers for the encapsulation of hydrophobic molecules, such as oleanolic acid. In general, however, the size and morphology of polymer self-assemblies of this kind (e.g., spherical and cylindrical micelles, vesicles, and single- and multi-chain polymer nanoparticles) depend on their specific molecular architecture [26]. For example, the ratio between the hydrophobic and hydrophilic blocks is crucial in this context [26,46]. Indeed, simulations demonstrate that the molecular structure of amphiphilic block copolymers plays a critical role in the formation of aggregates, particularly regarding the size of the hydrophobic and hydrophilic segments, namely the amphiphile's surface area, the volume and maximum effective length of the hydrophobic chain [26]. The self-assembly behavior of these systems is also affected by the polymer concentration, as well as the concentration and type of other species (e.g., metal ions [46]). Consequently, various approaches are being considered to fine-tune the properties of these advanced materials, including their mechanical properties [47]. Therefore, further refinement of the ATRP and RAFT reaction conditions proposed in this work may be considered to enable even more precise tailoring of the molecular architecture of the p(GMA-OA)-*b*-p(DMAEMA) copolymers, with the aim of designing nano-carriers that exhibit improved features compared to those shown in Fig. 13. Various techniques (e.g., solvent-switch approach, polymer rehydration, etc., [26]) and working conditions (e.g., polymer concentrations) may also be employed to customize these nanostructures.

Table 7
Brief comparison of the different synthetic approaches considered in this study for the incorporation of oleic acid in amphiphilic block copolymers through the reaction with glycidyl methacrylate.

Reaction route	Observations
Synthesis of methacrylated oleic acid from glycidyl methacrylate and oleic acid, followed by ATRP/RAFT polymerization	Difficult due to branching/crosslinking, low ATRP/RAFT polymerization yield, low solubility in successive steps leading to p(GMA-OA)-*b*-p(DMAEMA)
Incorporation of oleic acid in ATRP/RAFT p(GMA) homopolymers followed by polymerization with DMAEMA	Limited solubility of the p(GMA-OA) products hindering the incorporating the p(DMAEMA) block
Incorporation of oleic acid in ATRP/RAFT p(GMA)-*b*-p(DMAEMA) copolymers	p(GMA-OA)-*b*-p(DMAEMA) was achieved and self-assembly in well-defined spherical aggregates was observed
Simultaneous ATRP attachment of the p(DMAEMA) block and incorporation of oleic acid in p(GMA) homopolymers	p(GMA-OA)-*b*-p(DMAEMA) was achieved and self-assembly in well-defined spherical aggregates was observed. Hard removal of OA in excess

3.6. Application with encapsulation and delivery of oleanolic acid

Oleanolic acid is a pentacyclic triterpenoid found in many plants, including the olive tree, where it occurs alongside oleic acid. Notably, triterpenoids such as oleanolic and maslinic acids have been investigated for use in medicinal chemistry due to their antiproliferative and apoptosis-inducing effects on cancer cells, as well as their potential in HIV chemotherapy and other biological applications [48–58]. However, oleanolic acid is poorly soluble in water (estimated solubility ~4.6 mg/L at 20 °C) and is poorly absorbed from the gastrointestinal tract (permeability ~10^{-6} cm/s), resulting in an absolute oral bioavailability of around 0.7 % for doses of 25 and 50 mg/kg [48,52]. Therefore, many researchers are focusing on developing delivery systems for oleanolic acid in order to enhance its bioavailability and improve the efficacy of

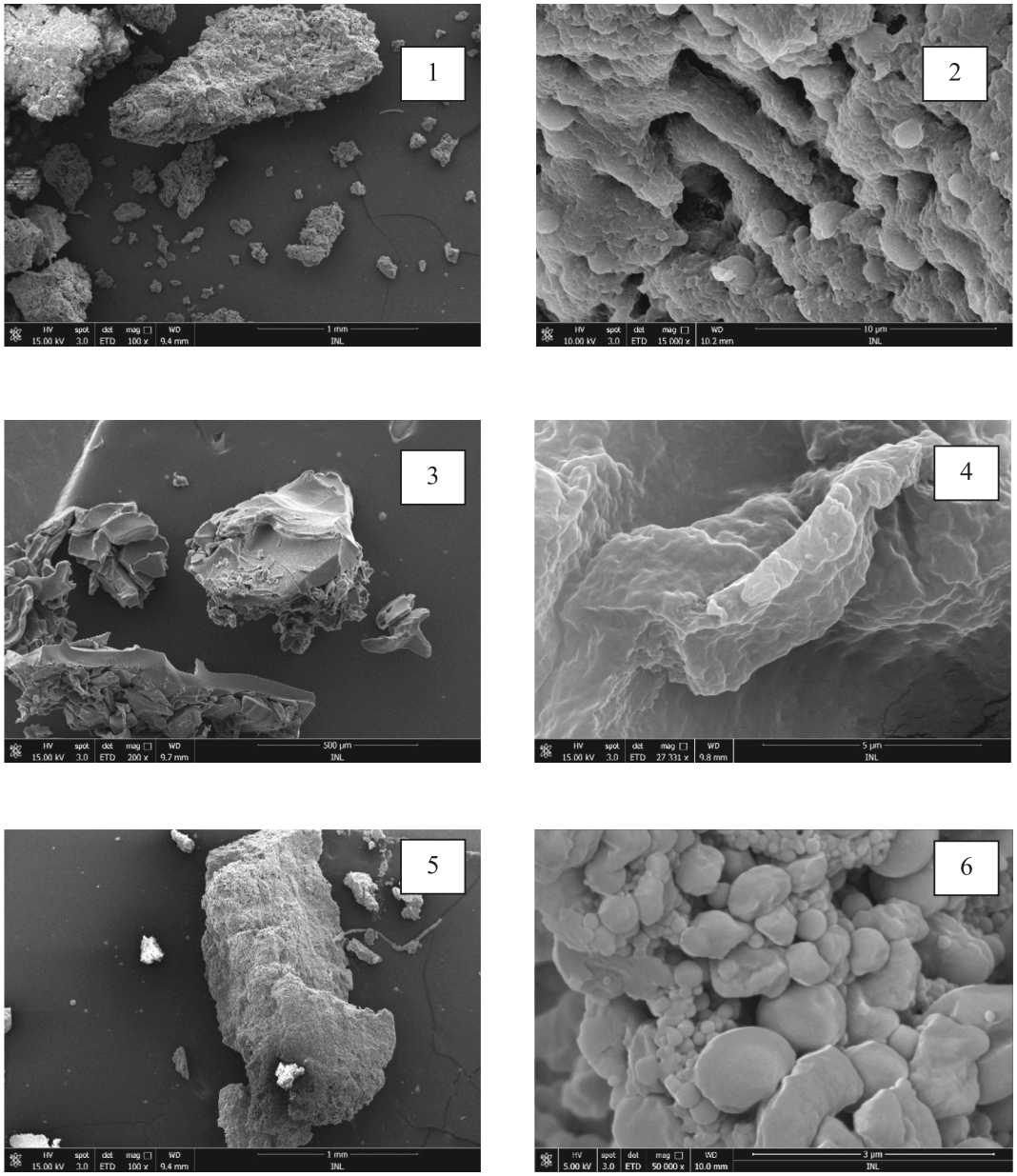

Fig. 12. SEM images of solid particles of the p(GMA-OA)-*b*-p(DMAEMA) copolymers synthesized in this research. 1 and 2 – OAP1, 3 and 4 – OAP2, 5 and 6 – OAP4.

therapies. In this context, it is especially important to consider controlled drug delivery systems, which aim to transport drugs directly to target sites while minimizing side effects and reducing the required dosage. Attempts to increase the solubility of oleanolic acid in water have included using solid dispersions, compounding with β-cyclodextrin, and changing the crystal form using spray drying, among other methods. Conversely, the main drug delivery systems that have been explored for the controlled delivery of oleanolic acid are solid lipid nanoparticles, liposomes, microemulsions, nanodispersions, phospholipid complexes, nanostructured lipid carriers, nanoparticles and micelles [52]. Tailored drug delivery systems offer significant advantages over traditional plant-active formulations. These include the potential for intracellular uptake, sustained release and protection against physical and chemical degradation [52]. Polymers play a key role in the development of such kinds of drug delivery systems for oleanolic acid, specifically as carriers in solid dispersions and as components for microemulsions, nanodispersions, nanoparticles or micelles.

Following this line of thought, the encapsulation and delivery of oleanolic acid using the developed p(GMA-OA)-*b*-p(DMAEMA) copolymers is here analyzed. The low aqueous solubility and limited permeability of oleanolic acid result from the presence of nonpolar functional groups in its structure, specifically the hydrophobic regions of the bulky ring structures characteristic of pentacyclic triterpenoids. The current approach explores the possibility of a strong hydrophobic interaction between the oleic acid moieties incorporated into the p(GMA-OA)-*b*-p(DMAEMA) copolymers and oleanolic acid (see scheme S2 depicted in SI). These hydrophobic interactions are believed to facilitate the encapsulation of oleanolic acid in an aqueous environment. The hydrophilic functional groups in the DMAEMA moieties act as the hydrophobic/hydrophilic interface. Simple visual confirmation of the ability of p(GMA-OA)-*b*-p(DMAEMA) copolymers to encapsulate hydrophobic compounds was obtained using Nile Red as a model molecule. Indeed, a color change was observed as the surrounding solvent was varied, starting with a mixture of Nile Red and p(GMA-OA)-*b*-p(DMAEMA) in THF and approaching an aqueous environment through a dialysis process in a cellulose bag (see Fig. S14 in SI). This color change

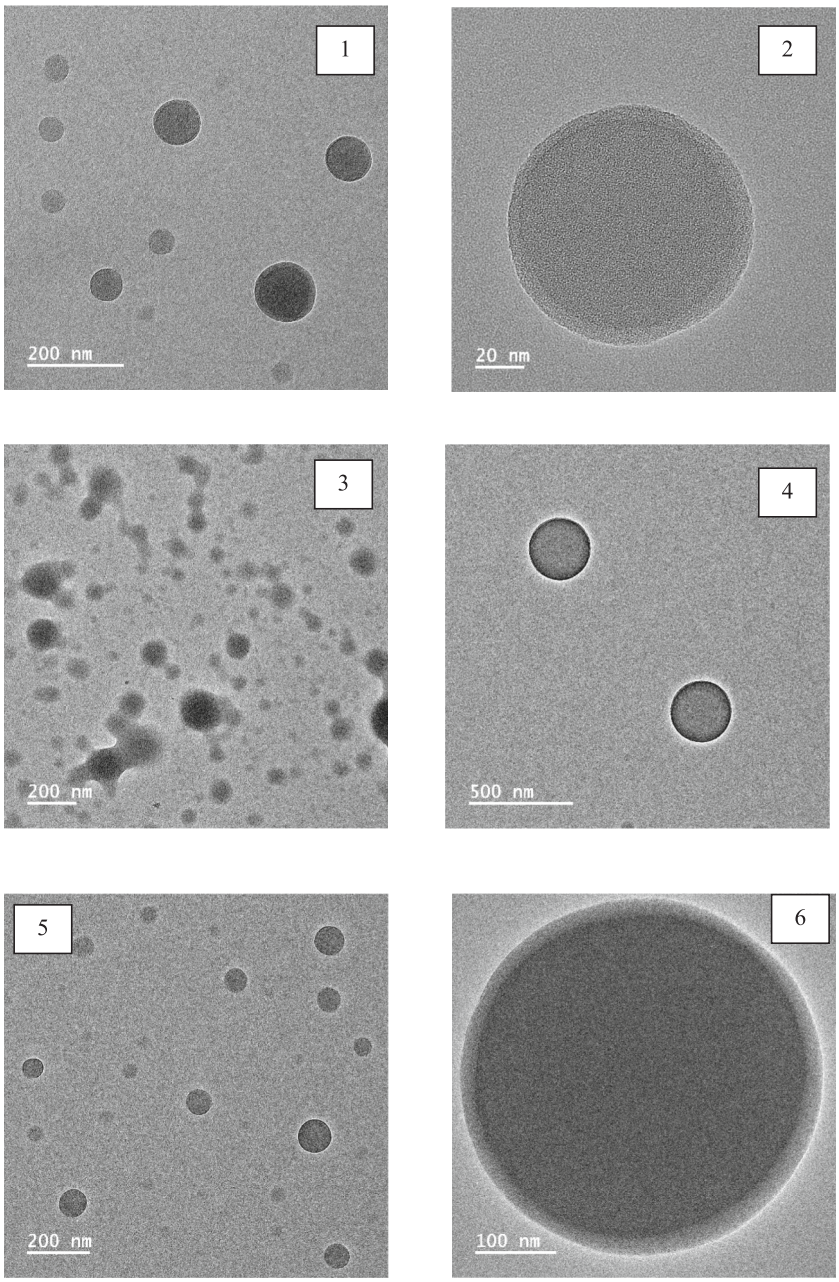

Fig. 13. TEM images of aqueous dispersions produced with different p(GMA-OA)-*b*-p(DMAEMA) copolymers synthesized in this research. 1 and 2 – OAP1, 3 – OAP2, 4 – OAP3, 5 and 6 – OAP4 (see Table 5).

indicates the encapsulation of Nile Red within the hydrophobic portion of the p(GMA-OA)-*b*-p(DMAEMA) aggregates, specifically the OA-containing moieties.

Encapsulation of oleanolic acid in solid dispersions was performed using p(GMA-OA)-*b*-p(DMAEMA) materials as a polymeric carrier and a solvent evaporation method with THF. On the other hand, micro-emulsions/nanodispersions with encapsulated oleanolic acid were also prepared using p(GMA-OA)-*b*-p(DMAEMA) through dispersion in THF followed by dialysis in cellulose bag (see experimental section). Precipitation of material during transition to an aqueous environment was observed to a small extent, namely with OAP1, indicating that the formation of polymer chains that are not suitable for self-assembly is plausible. As discussed above, the presence of free p(DMAEMA) is possible in the case of OAP1. In both cases, the amount of oleanolic acid encapsulated was estimated by dispersing the solid particles in a large excess of methanol [53], followed by HPLC-DAD analysis of the resulting liquid phase (see the quantification of oleanolic acid by HPLC-DAD in the SI, Fig. S17). Concentrations of oleanolic acid in solid dispersions were observed to be up to 0.21 mg/mg, while concentrations in particle dispersions were estimated to be up to 0.17 mg/mL.

Dried solid particles and dispersions of p(GMA-OA)-*b*-p(DMAEMA) with oleanolic acid encapsulated where thereafter scrutinized as drug delivery systems, specifically concerning the dynamics of oleanolic acid release. Following recent related studies, EtOH/PBS 30/70 was considered as the reference medium for oleanolic acid release [53]. Solid particles were directly dispersed in EtOH/PBS 30/70 while aqueous dispersions were dialyzed against EtOH/PBS 30/70. In both cases, the liquid phase was sampled along the time (exterior of dialysis bag with dispersions) for HPLC-DAD quantification of the contained oleanolic acid. Fig. 14 shows the dynamics of oleanolic acid release that were measured under these conditions. A logarithmic scale is used to represent the fraction of released oleanolic acid, which highlights the

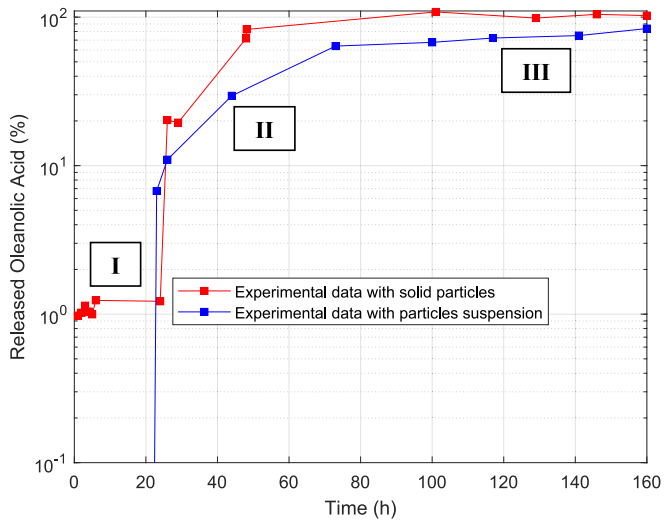

Fig. 14. Measured dynamics of oleanolic acid release from encapsulation solid particles and particle dispersions of copolymers of p(GMA-OA)-*b*-p(DMAEMA). The composition of the release fluid was changed along the time according to the following: **I** – EtOH/PBS 30/70, **II** – (EtOH/PBS 30/70)/MeOH 50/50, **III** – (EtOH/PBS 30/70)/MeOH 20/80. Experiments with PBS solution at pH = 7.6 and T = 25 °C. The concentration of oleanolic acid in the release fluid was measured by HPLC-DAD. Log scale is used to represent the released oleanolic acid, highlighting the observed differences in magnitude.

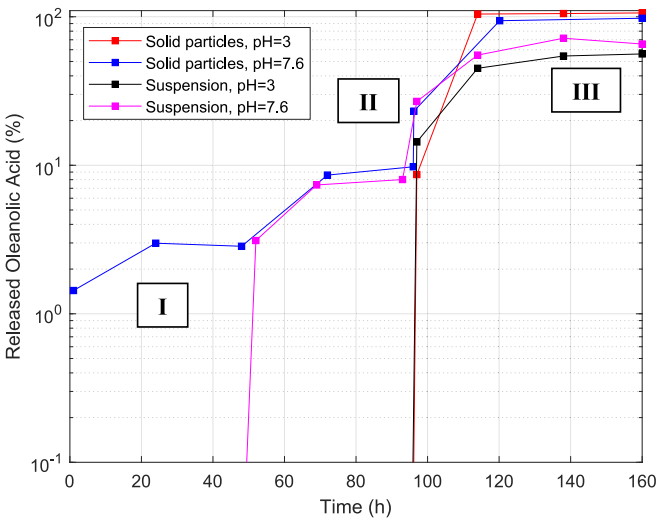

Fig. 15. Measured dynamics of oleanolic acid release from encapsulation solid particles and particle dispersions of copolymers of p(GMA-OA)-*b*-p(DMAEMA). The composition of the release fluid was changed along the time according to the following: I – EtOH/buffer 30/70, II – (EtOH/buffer 30/70)/MeOH 50/50, III – (EtOH/buffer 30/70)/MeOH 20/80. Experiments with PBS solution at pH = 7.6 and acetate buffer at pH = 3. All the experiments at T = 40 °C. The concentration of oleanolic acid in the release fluid was measured by HPLC-DAD. Log scale is used to represent the released oleanolic acid, highlighting the observed differences in magnitude.

differences in magnitude observed for the various surrounding conditions (constant temperature of 25 °C). Indeed, a sustained release of oleanolic acid is observed in EtOH/PBS 30/70 for at least 24 h (region **I**). For solid particles, a steady value for OA delivery of around 1 % (concentration in the liquid ~6 mg/L) is observed, while for aqueous dispersions in the same conditions, a negligible value of less than 0.1 % is estimated (note the impact of diffusion through the cellulose bag on this system). To demonstrate the high amount of oleanolic acid encapsulated in the particles, the release was triggered by altering the composition of the surrounding liquid phase. This was achieved by adding methanol to the system to create a mixture of (EtOH/PBS 30/70)/MeOH 50/50 (region **II**). A substantial increase in oleanolic acid release was observed, with measured values ranging over the time from 20 to 70 % for solid particles, and from 7 to 30 % for dispersions. An additional delivery stage was induced by the further addition of methanol, which changed the composition of the liquid phase to (EtOH/PBS 30/70)/MeOH 20/80 (region **III**). The amount released was found to approach 100 % for the solid particles, while a steady value of around 70 % was achieved with the dispersion.

To assess the potential impact of pH on oleanolic acid release due to the presence of DMAEMA moieties in the p(GMA-OA)-*b*-p(DMAEMA) copolymers used for encapsulation, experiments involving fluids at pH 3 and 7.6 were conducted. The temperature was also increased to 40 °C because p(DMAEMA) is thermoresponsive with lower critical solution temperature (LCST) at around 50 °C (aggregation observed because of hydrogen bond disruption). An acetate buffer was used to achieve a pH of 3, while a PBS buffer was used to achieve a pH of 7.6. Fig. 15 presents the results obtained under these conditions, showing a significant difference in oleanolic acid release for both solid particles and dispersions when the pH of the surrounding fluid is varied. Indeed, a faster release dynamic is observed with both solid particles and dispersions when the surrounding pH is 7.6, compared with the corresponding delivery profiles at pH 3. This is highlighted in Fig. 15 during regime **I**, where EtOH/buffer 30/70 was used. Note the negligible release of oleanolic acid at pH 3 over a period of up to around 100 h, for both solid particles and dispersions. Notably, the morphology of the polymer particles and dispersion stability is also affected by the pH, with observation of swelled material at pH 3 and collapsing of the material at pH 7.6, as showed in images S15 and S16 of the SI. These observations confirm the pH responsiveness of the copolymers, which is consistent with the expected behavior induced by p(DMAEMA): swelling in acidic conditions and collapsing at alkaline pH due to ionization and deionization, respectively. The lower amount of oleanolic acid released in acidic conditions (pH 3) is likely due to the low ionization of this compound compared to pH 7.6, resulting in reduced solubility in the surrounding fluid. The confirmation for a substantial additional amount of oleanolic acid encapsulated in the solid particles and dispersions was again worked out by changing the composition of the release fluid through the addition of methanol. The correspondent results are also presented in Fig. 15 with the inclusion of region **II** (fluid composition (EtOH/buffer 30/70)/MeOH 50/50) and **III** (fluid composition (EtOH/buffer 30/70)/MeOH 20/80). Note the relevant boost in oleanolic acid release observed in these regions even for the systems with the initial use of EtOH/buffer 30/70 at pH 3. This is a consequence of the increase of solubility of oleanolic acid in the surround fluid when methanol is added, thus confirming the potential of the encapsulation vehicles to deliver high amounts of this molecule. In region **III** (highest composition in methanol) similar release fractions are observed for the initial systems at pH 3 and pH 7.6, approaching 100 % for both solid particles and 70 % for both dispersions.

4. Conclusion

This research focused on assessing different reaction routes using glycidyl methacrylate to synthesize amphiphilic block copolymers that incorporate oleic acid in the hydrophobic part. The hydrophilic segment was built up with the 2-(dimethylamino)ethyl methacrylate monomer. The main goals of this work were to find reaction routes that lead to low-impact branching and/or crosslinking mechanisms involving epoxides and oleic acid, and to synthesize p(GMA-OA)-*b*-p(DMAEMA) copolymers in a straightforward and scalable way. The synthesis of block copolymers was considered using both ATRP and RAFT polymerization.

The reaction route involving the synthesis of methacrylated oleic acid from glycidyl methacrylate and oleic acid proved problematic due to branching/crosslinking, a low ATRP/RAFT polymerization yield, and

the difficulty of solubilizing the reactants in successive steps, resulting in p(GMA-OA)-*b*-p(DMAEMA) copolymers. However, higher synthesis efficiency was observed when glycidyl methacrylate moieties were modified by post-polymerization with oleic acid. This research identified the following routes for efficiently synthesizing the desired p(GMA-OA)-*b*-p(DMAEMA) materials:

a) RAFT or ATRP synthesis of the p(GMA) block, followed by attachment of the p(DMAEMA) block and final incorporation of oleic acid into the p(GMA)-*b*-p(DMAEMA) block copolymers to produce the desired p(GMA-OA)-*b*-p(DMAEMA) material.
b) ATRP synthesis of the p(GMA) block, followed by simultaneous attachment of the p(DMAEMA) block and incorporation of oleic acid to get the p(GMA-OA)-*b*-p(DMAEMA) material.

Working with DMSO solvent and a stoichiometric excess of oleic acid compared to epoxide groups was found to be particularly important for reducing branching and crosslinking during the step involving the incorporation of oleic acid into the copolymers. FTIR and GPC analyses were used to assess the progress of the chemical composition and molecular architecture of the intermediate homo- and *co*-polymers, and to demonstrate the successful production of the intended p(GMA-OA)-*b*-p(DMAEMA) materials. FTIR analysis demonstrated the total conversion of epoxides through reaction with oleic acid. The synthesized amphiphilic block copolymers were considered as a potential vehicle for encapsulating and delivering oleanolic acid, a pentacyclic triterpenoid that is found in many plants, including the olive tree, where it occurs alongside oleic acid. SEM and TEM analyses were performed to elucidate the morphology of these vehicles when considering the use of solid polymer dispersions and aqueous dispersions for encapsulating and delivering oleanolic acid. The ability of the p(GMA-OA)-*b*-p(DMAEMA) copolymers to self-assemble in an aqueous environment was demonstrated by observing nano-dispersions, including well-defined spherical particles up to ~100 nm in size with an external shell around 5–8 nm thick. Spherical aggregates with a size of up to ~500 nm were observed in aqueous dispersions when using a p(GMA-OA)-*b*-p(DMAEMA) copolymer synthesized through the simultaneous attachment of the DMAEMA block and the incorporation of oleic acid. The loading capacity of oleanolic acid was estimated to be 0.21 mg/mg in solid polymer dispersions, and 0.17 mg/mL in aqueous particle dispersions. These are relevant values when considering the use of the materials to release oleanolic acid in aqueous environments. The dynamics of oleanolic acid release was measured under different conditions, including changes in solvent composition, pH and temperature. The results demonstrate sustained release of the encapsulated oleanolic acid and morphological transitions induced by pH/temperature changes due to the ionization/deionization of the tertiary amines contained within the hydrophilic p(DMAEMA) domain in acidic/alkaline conditions.

Overall, the proposed synthesis routes lead to the efficient formation of amphiphilic copolymers of the type p(GMA-OA)-*b*-p(DMAEMA), thus creating hybrid natural-synthetic tailored materials. These copolymers are capable of self-assembling in an aqueous environment to form nano-carriers that can encapsulate hydrophobic molecules such as oleanolic acid. Further refinement of the ATRP and RAFT reaction conditions presented in this work could improve the tailoring of the molecular architecture of the p(GMA-OA)-*b*-p(DMAEMA) copolymers and customization of nano-carriers, including their mechanical properties and drug release capabilities. Various alternative techniques (e.g., solvent-switch approach, polymer rehydration, etc.,) and working conditions, such as the polymer concentration and formulation of the dispersion, may also be employed to customize these nanostructures. The application of the class of amphiphilic copolymers here developed to the sustained release of other kinds of natural hydrophobic molecules, namely related pentacyclic triterpenoids with proved therapeutic effects, such as maslinic acid or betulinic acid, is also another future promising line of research in this area.

CRediT authorship contribution statement

Catarina P. Gomes: Writing – original draft, Methodology, Investigation, Conceptualization. **Mário Rui P.F.N. Costa:** Writing – review & editing, Investigation, Conceptualization. **Rolando C.S. Dias:** Writing – review & editing, Supervision, Funding acquisition, Conceptualization.

Declaration of competing interest

The authors declare that they have no known competing financial interests or personal relationships that could have appeared to influence the work reported in this paper.

Acknowledgments

Catarina Gomes acknowledges to FCT for the PhD scholarship 2020.06057.BD. Rolando Dias is grateful to the Foundation for Science and Technology (FCT, Portugal) for financial support through national funds FCT/MCTES (PIDDAC) to CIMO (UIDB/00690/2020 and UIDP/00690/2020) and SusTEC (LA/P/0007/2020). Mário Rui Costa acknowledges the support by LA/P/0045/2020 (ALiCE), UIDB/50020/2020 and UIDP/50020/2020 (LSRE-LCM), funded by national funds through FCT/MCTES (PIDDAC).

Appendix A. Supplementary data

Supplementary data to this article can be found online at https://doi.org/10.1016/j.reactfunctpolym.2025.106492.

Data availability

The data are available from the authors on request.

References

[1] M. Benaglia, A. Alberti, L. Giorgini, F. Magnonia, S. Tozzia, Poly(glycidyl methacrylate): a highly versatile polymeric building block for post-polymerization modifications, Polym. Chem. 4 (2013) 124, https://doi.org/10.1039/c2py20646c.
[2] M. Moreno, J.I. Miranda, M. Goikoetxea, M.J. Barandiaran, Sustainable polymer latexes based on linoleic acid for coatings applications, Prog. Org. Coat. 77 (2014) 1709–1714, https://doi.org/10.1016/j.porgcoat.2014.05.016.
[3] E. Can, J.J. La Scala, J.M. Sands, G.R. Palmese, The synthesis of 9–10 Dibromo stearic acid glycidyl methacrylate and its use in vinyl ester resins, J. Appl. Polym. Sci. 106 (2007) 3833–3842, https://doi.org/10.1002/app.26249.
[4] M. Moreno, M. Goikoetxea, M.J. Barandiaran, Biobased-waterborne homopolymers from oleic acid derivatives, J. Polym. Sci. A Polym. Chem. 50 (2012) 4628–4637, https://doi.org/10.1002/pola.26287.
[5] S.H. Li, X.J. Yang, K. Huang, M. Li, J.L. Xia, Preparation and characterization of dimer fatty acids-based vinyl ester resin monomer, AMR 721 (2013) 86–89, https://doi.org/10.4028/www.scientific.net/amr.721.86.
[6] T. Dey, Properties of vinyl ester resins containing methacrylated fatty acid comonomer: the effect of fatty acid chain length, Polym. Int. 56 (2007) 853–859, https://doi.org/10.1002/pi.2215.
[7] G.R. Palmese, J.J. La Scala, J.M. Sands, Fatty Acid Monomers to Reduce Emissions and Toughen Polymers, Patent US008372926B2. https://patentimages.storage.googleapis.com/d9/20/38/290359475055ed/US8372926.pdf, 2013.
[8] G. Capiel, N.E. Marcovich, M.A. Mosiewicki, From the synthesis and characterization of methacrylated fatty acid based precursors to shape memory polymers, Polym. Int. 68 (2019) 546–554, https://doi.org/10.1002/pi.5744.
[9] G. Capiel, N.E. Marcovich, M.A. Mosiewicki, Shape memory polymer networks based on methacrylated fatty acids, Eur. Polym. J. 116 (2019) 321–329, https://doi.org/10.1016/j.eurpolymj.2019.04.023.
[10] M. Decostanzi, J. Lomège, Y. Ecochard, Anne-S. Mora, C. Negrell, S. Caillol, Fatty acid-based cross-linkable polymethacrylate coatings, Prog. Org. Coat. 124 (2018) 147–157, https://doi.org/10.1016/j.porgcoat.2018.08.001.
[11] J. Lomège, V. Lapinte, C. Negrell, Jean-J. Robin, S. Caillol, Fatty acid-based radically polymerizable monomers: from novel poly(meth)acrylates to cutting-edge properties, Biomacromolecules 20 (2019) 1525–7797, https://doi.org/10.1021/acs.biomac.8b01156.
[12] E.M. Muzammil, A. Khan, M.C. Stuparu, Post-polymerization modification reactions of poly(glycidyl methacrylate)s, RSC Adv. 7 (2017) 55874, https://doi.org/10.1039/c7ra11093f.
[13] M. Petro, F. Svec, J.M.J. Fréchet, Monodisperse hydrolyzed poly(glycidyl methacrylate-co-ethylene dimethacrylate) beads as a stationary phase for normal-

phase HPLC, Anal. Chem. 69 (1997) 3131–3139, https://doi.org/10.1021/ac970365a.
[14] E. Suárez, B. Paredes, F. Rubiera, M. Rendueles, M.A. Villa-García, J.M. Díaz, Functionalized glycidyl methacrylate based polymers as stationary phases for protein retention, Sep. Purif. Technol. 27 (2002) 1–10, https://doi.org/10.1016/S1383-5866(01)00163-0.
[15] S. Li, Z. Li, F. Zhang, H. Geng, B. Yang, A polymer-based zwitterionic stationary phase for hydrophilic interaction chromatography, Talanta 216 (2020) 120927, https://doi.org/10.1016/j.talanta.2020.120927.
[16] A.N. Tasfiyati, E.D. Iftitah, S.P. Sakti, A. Sabarudin, Evaluation of glycidyl methacrylate-based monolith functionalized with weak anion exchange moiety inside 0.5 mm i.d. column for liquid chromatographic separation of DNA, Anal. Chem. Res. 7 (2016) 9–16, https://doi.org/10.1016/j.ancr.2015.11.001.
[17] D. Poddar, A. Singh, S. Bansal, S. Thakur, P. Jain, Direct synthesis of poly(Ɛ-caprolactone)-block-poly (glycidyl methacrylate) copolymer and its usage as a potential nano micelles carrier for hydrophobic drugs, J. Indian Chem. Soc. 99 (2022) 100537, https://doi.org/10.1016/j.jics.2022.100537.
[18] J. Ma, M. Li, L. Sun, B. Nie, C. Cao, Preparation of amphiphilic block copolymers via RAFT polymerization and preliminary properties exploration of blended membranes with PVDF, J. Polym. Res. 31 (2024) 282, https://doi.org/10.1007/s10965-024-04112-2.
[19] S.A. Mohammad, D. Kumar, M.M. Alam, S. Banerjee, Ultrafast, green and recyclable photoRDRP in an ionic liquid towards multi-stimuli responsive amphiphilic copolymers, Polym. Chem. 12 (2021) 4954, https://doi.org/10.1039/D1PY01014J.
[20] L. Leemans, R. Fayt, P. Teyssié, Synthesis of new amphiphilic block copolymers. Block copolymer of sulfonated glycidyl methacrylate and alkyl methacrylate, J. Polym. Sci. A Polym. Chem. 28 (1990) 1255–1262, https://doi.org/10.1002/pola.1990.080280524.
[21] L. Shechter, J. Wynstra, Glycidyl ether reactions with alcohols, phenols, carboxylic acids, and acid anhydrides, Ind. Eng. Chem. 48 (1956) 86–93, https://doi.org/10.1021/ie50553a028.
[22] S. Oliver, O. Vittorio, G. Cirillo, C. Boyer, Enhancing the therapeutic effects of polyphenols with macromolecules, Polym. Chem. 7 (2016) 1529–1544, https://doi.org/10.1039/c5py01912e.
[23] M.A. Beach, U. Nayanathara, Y. Gao, C. Zhang, Y. Xiong, Y. Wang, G.K. Such, Polymeric nanoparticles for drug delivery, Chem. Rev. 124 (2024) 5505–5616, https://doi.org/10.1021/acs.chemrev.3c00705.
[24] M.C. Pereira, L.E. Hill, R.C. Zambiazi, S. Mertens-Talcott, S. Talcott, C.L. Gomes, Nanoencapsulation of hydrophobic phytochemicals using poly (dl-lactide-co-glycolide) (PLGA) for antioxidant and antimicrobial delivery applications: Guabiroba fruit (Campomanesia xanthocarpa O. Berg) study, LWT Food Sci. Technol. 63 (2015) 100–107, https://doi.org/10.1016/j.lwt.2015.03.062.
[25] R. Ahmad, S. Srivastava, S. Ghosh, S.K. Khare, Phytochemical delivery through nanocarriers: a review, Colloids Surf. B: Biointerfaces 197 (2021) 111389, https://doi.org/10.1016/j.colsurfb.2020.111389.
[26] C.P. Gomes, A. Bzainia, R.C.S. Dias, M.R.P.F.N. Costa, Polymersomes as versatile drug delivery vesicular carriers, in: Systems of Nanovesicular Drug Delivery, Elsevier, 2022, https://doi.org/10.1016/B978-0-323-91864-0.00018-8.
[27] A. Bzainia, C.P. Gomes, R.C.S. Dias, M.R.P.F.N. Costa, Molecular imprinting and surface grafting of glycoprotein fragments in polymeric nanosystems: from cancer diagnosis to virus targeting, in: Polymeric Nanosystems, Elsevier, 2023, https://doi.org/10.1016/B978-0-323-85656-0.00012-7.
[28] D. Xiao, H. Wu, Y. Zhang, J. Kang, A. Dong, W. Liang, Advances in stimuli-responsive systems for pesticides delivery: recent efforts and future outlook, J. Control. Release 352 (2022) 288–312, https://doi.org/10.1016/j.jconrel.2022.10.028.
[29] M. Yadav, Nanoparticle-facilitated targeted nutrient delivery in plants: breakthroughs and mechanistic insights, Plant Nano Biol. 12 (2025) 100156, https://doi.org/10.1016/j.plana.2025.100156.
[30] A. Zanino, F. Pizzetti, M. Masi, F. Rossi, Polymers as controlled delivery systems in agriculture: the case of atrazine and other pesticides, Eur. Polym. J. 203 (2024) 112665, https://doi.org/10.1016/j.eurpolymj.2023.112665.
[31] R. Wang, S. Liu, Z. Ma, Recent development of versatile polyphenol platforms in fertilizers and pesticides, J. Agric. Food Chem. 71 (2023) 9599–9608, https://doi.org/10.1021/acs.jafc.3c01952.
[32] C.P. Gomes, R.C.S. Dias, M.R.P.F.N. Costa, Hybrid cellulose-poly(4-vinylpyridine) adsorbents produced via ATRP and their application to target polyphenols in winemaking, olive oil production and almond processing residues, React. Funct. Polym. 164 (2021) 104930, https://doi.org/10.1016/j.reactfunctpolym.2021.104930.
[33] C.P. Gomes, R.C.S. Dias, M.R.P.F.N. Costa, Surface molecularly imprinted cellulose-synthetic hybrid particles prepared via ATRP for enrichment of flavonoids in olive leaf, Macromol. React. Eng. 17 (2023) 2300011, https://doi.org/10.1002/mren.202300011.
[34] A. Almeida, R.M. Gaspar, S. Ferreira-Dias, M.R.P.F.N. Costa, R.C.S. Dias, Pyridyl-functionalized and surface molecularly imprinted cellulose particles to target bioactive compounds in olive leaf, React. Funct. Polym. 214 (2025) 106338, https://doi.org/10.1016/j.reactfunctpolym.2025.106338.
[35] C.S. Gudipati, M.B.H. Tan, H. Hussain, Y. Liu, C. He, T.P. Davis, Synthesis of poly (glycidyl methacrylate)-block-poly(pentafluorostyrene) by RAFT: precursor to novel amphiphilic poly(glyceryl methacrylate)-block-poly(pentafluorostyrene), Macromol. Rapid Commun. 29 (2008) 1902–1907, https://doi.org/10.1002/marc.200800515.
[36] J. Zhu, D. Zhou, X. Zhu, G. Chen, Reversible addition–fragmentation chain transfer polymerization of glycidyl methacrylate with 2-cyanoprop-2-yl 1-dithionaphthalate as a chain-transfer agent, J. Polym. Sci. A Polym. Chem. 42 (2004) 2558–2565, https://doi.org/10.1002/pola.20119.
[37] N. Ezaki, Y. Watanabe, H. Mori, Amphiphilic block-random copolymer surfactants with tunable hydrophilic/hydrophobic balance for preparation of non-aqueous dispersions by an emulsion solvent evaporation method, React. Funct. Polym. 110 (2017) 10–20, https://doi.org/10.1016/j.reactfunctpolym.2016.11.004.
[38] J. Sáncheza, C. Espinosa, F. Pooch, H. Tenhu, G.C. del Pizarro, D.P. Oyarzún, Poly (N,N-dimethylaminoethyl methacrylate) for removing chromium (VI) through polymer-enhanced ultrafiltration technique, React. Funct. Polym. 127 (2018) 67–73, https://doi.org/10.1016/j.reactfunctpolym.2018.04.002.
[39] N. Pantoustier, S. Moins, M. Wautier, P. Degée, P. Dubois, Solvent-free synthesis and purification of poly[2-(dimethylamino)ethyl methacrylate] by atom transfer radical polymerization, Chem. Commun. 3 (2003) 340–341, https://doi.org/10.1039/B208703K.
[40] G. Li, X. Zhu, J. Zhu, Z. Cheng, W. Zhang, Homogeneous reverse atom transfer radical polymerization of glycidyl methacrylate and ring-opening reaction of the pendant oxirane ring, Polymer 46 (2005) 12716–12721, https://doi.org/10.1016/j.polymer.2005.10.061.
[41] A. Hayek, Y. Xu, T. Okada, S. Barlow, X. Zhu, J.H. Moon, S.R. Marder, S. Yang, Poly (glycidyl methacrylate)s with controlled molecular weights as low-shrinkage resins for 3D multibeam interference lithography, J. Mater. Chem. 18 (2008) 3316–3318, https://doi.org/10.1039/B809656B.
[42] K. Matyjaszewski, S. Coca, C.B. Jasieczek, Polymerization of acrylates by atom transfer radical polymerization. Homopolymerization of glycidyl acrylate, Macromol. Chem. Phys. 198 (1997) 4011–4017, https://doi.org/10.1002/macp.1997.021981219.
[43] R. Krishnan, K.S.V. Srinivasan, Controlled/"living" radical polymerization of glycidyl methacrylate at ambient temperature, Macromolecules 36 (2003) 1769–1771, https://doi.org/10.1021/ma025637c.
[44] H.A. Afzala, R.V. Ghorpadeb, A.K. Thorveb, S. Nagarajac, B.E. Al-Dhubiabc, G. Meravaniged, S.T. Rasoole, T.S. Roopashreef, Epoxy functionalized polymer grafted magnetic nanoparticles by facile surface initiated polymerization for immobilization studies of Candida Antarctica lipase B, React. Funct. Polym. 147 (2020) 104454, https://doi.org/10.1016/j.reactfunctpolym.2019.104454.
[45] S.Á. de Gonçalves, R.P. Vieira, Current status of ATRP-based materials for gene therapy, React. Funct. Polym. 147 (2020) 104453, https://doi.org/10.1016/j.reactfunctpolym.2019.104453.
[46] Y. Man, X. Li, S. Li, Z. Yang, Y.-I. Lee, H.-G. Liu, Effects of hydrophobic/hydrophilic blocks ratio on PS-b-PAA self-assembly in solutions, in emulsions, and at the interfaces, Colloids Surf. A Physicochem. Eng. Asp. 580 (2019) 123684, https://doi.org/10.1016/j.colsurfa.2019.123684.
[47] F. Perin, A. Motta, D. Maniglio, Amphiphilic copolymers in biomedical applications: synthesis routes and property control, Mater. Sci. Eng. C 123 (2021) 111952, https://doi.org/10.1016/j.msec.2021.111952.
[48] Q. Jiang, X. Yang, P. Du, H. Zhang, T. Zhang, Dual strategies to improve oral bioavailability of oleanolic acid: enhancing water-solubility, permeability and inhibiting cytochrome P450 isozymes, Eur. J. Pharm. Biopharm. 99 (2016) 65–72, https://doi.org/10.1016/j.ejpb.2015.11.013.
[49] J. Liu, Oleanolic acid and ursolic acid: research perspectives, J. Ethnopharmacol. 100 (2005) 92–94, https://doi.org/10.1016/j.jep.2005.05.024.
[50] D.W. Jeong, Y.H. Kim, H.H. Kim, H.Y. Ji, S.D. Yoo, W.R. Choi, S.M. Lee, C.-K. Han, H.S. Lee, Dose-linear pharmacokinetics of oleanolic acid after intravenous and oral administration in rats, Biopharm. Drug Dispos. 28 (2007) 51–57, https://doi.org/10.1002/bdd.530.
[51] M. Vasarri, M.C. Bergonzi, M. Leri, R. Castellacci, M. Bucciantini, L. De Marchi, D. Degl'Innocenti, Protective effects of oleanolic acid on human keratinocytes: a defense against exogenous damage, Pharmaceuticals 18 (2025) 238, https://doi.org/10.3390/ph18020238.
[52] M. Wasim, M.C. Bergonzi, Unlocking the potential of oleanolic acid: integrating pharmacological insights and advancements in delivery systems, Pharmaceutics 16 (2024) 692, https://doi.org/10.3390/pharmaceutics16060692.
[53] C. De Stefani, M. Vasarri, M.C. Salvatici, L. Grifoni, J.C. Quintela, A.R. Bilia, D. Degl'Innocenti, M.C. Bergonzi, Microemulsions enhance the in vitro antioxidant activity of oleanolic acid in RAW 264.7 cells, Pharmaceutics 14 (2022) 2232, https://doi.org/10.3390/pharmaceutics14102232.
[54] Y.-H. Yang, S.-Y. Dai, F.-H. Deng, L.-H. Peng, C. Li, Y.-H. Pei, Recent advances in medicinal chemistry of oleanolic acid derivatives, Phytochemistry 203 (2022) 113397, https://doi.org/10.1016/j.phytochem.2022.113397.
[55] M.E. Juan, J.M. Planas, V. Ruiz-Gutierrez, H. Daniel, U. Wenzel, Antiproliferative and apoptosis-inducing effects of maslinic and oleanolic acids, two pentacyclic triterpenes from olives, on HT-29 colon cancer cells, Br. J. Nutr. 100 (2008) 36, https://doi.org/10.1017/S0007114508882979.
[56] A.J. Vlietinck, T. DeBruyne, S. Apers, L.A. Pieters, Plant-derived leading compounds for chemotherapy of human immunodeficiency virus (HIV) infection, Planta Med. 64 (1998) 97–109, https://doi.org/10.1055/s-2006-957384.
[57] N. Gao, M. Guo, Q. Fu, Z. He, Application of hot melt extrusion to enhance the dissolution and oral bioavailability of oleanolic acid, Asian J. Pharm. Sci. 12 (2017) 66–72, https://doi.org/10.1016/j.ajps.2016.06.006.
[58] X. Yang, Q. Jiang, P. Du, J. Zhao, T. Zhang, Preparation and characterization of solidified oleanolic acid–phospholipid complex aiming to improve the dissolution of oleanolic acid, Asian J. Pharm. Sci. 11 (2016) 241–247, https://doi.org/10.1016/j.ajps.2015.07.002.